KfK 4076
EUR 9615e
Mai 1986

Fusion Technology Programme

Semi-annual Report Oktober 1985 - März 1986

Compiled by
D. Finken
Projekt Kernfusion

Kernforschungszentrum Karlsruhe

KERNFORSCHUNGSZENTRUM KARLSRUHE

Projekt Kernfusion

KfK 4076

EUR 9615 e

Fusion Technology Programme

Semi-annual Report

Oktober 1985 - März 1986

Compiled by
D. Finken

Kernforschungszentrum Karlsruhe GmbH, Karlsruhe

Kernforschungszentrum Karlsruhe GmbH
Postfach 3640, 7500 Karlsruhe 1

ISSN 0303-4003

CONTENTS

P r e f a c e

After steady progress of plasma physics experiments, in 1982, the magnetic fusion programme of the European Community was complemented by the NET (Next European Tokamak) and Technology Programme.
By this joint action of European Laboratories, technologies shall be developed needed to maintain a stable plasma burn and to extract energy for electricity production.

At this time, KfK joined the fusion programme of EURATOM as a further association introducing its experience in nuclear technology. KfK closely cooperates with IPP Garching, the two institutions forming a research unit aiming at planning and realization of future development steps of fusion.

KfK has combined its forces in the Nuclear Fusion Project (PKF) with participation of several KfK departments to the project tasks.

Previous work of KfK in magnetic fusion has addressed mainly superconducting magnets, plasma heating by cluster ions and studies on structural materials. At present, emphasis of our work has concentrated increasingly on the nuclear part, i.e. the first wall and blanket structures and the elements of the tritium extraction and purification system. Associated to this component development are studies of remote maintenance and safety.

Most of the actual work addresses NET, the next step to a demonstration of fusion feasibility. NET is supposed to follow JET, the operating plasma physics experiment of Euratom, in the 1990's. The NET design team at Garching is directly supported by KfK via delegation of 3 experts and by study contracts (about 10 myr/yr). Different from the study contracts, which are mostly short term actions launched by NET directly most of the work is organized in long term research agreements. These r+d contracts are proposed by NET, reviewed by expert groups and allocated to the associations by the Fusion Technology Steering Committee (FTSC) after a tendering procedure. The contracts are grouped in the following research areas:

- Blanket Development and Breeding Materials (B)
- First Wall and Shield Design (N)
- Superconducting Magnets (M)
- Tritium Technology (T)
- Structural Materials (MAT)
- Safety and Environment (S+E)
- Remote Maintenance (RM)

About 80 professional menyears per year are at present spent by KfK on participating to these technology tasks. In many cases, tasks are split between associations. Arrangements with partner laboratories range from complementarity of tasks to joint ventures. A particularly narrow cooperation has been established with CEA in blanket design, development of breeding materials and poloidal field coils.

As the programme advances and NET takes shape, the development work has to address more complex tasks in a coherent way. KfK is prepared to contribute increasingly in the areas of blanket engineering, tritium process techniques, magnet systems and safety studies.

Aside from the NET and Technology Programme, KfK conducts an experimental study on gyrotrons as a source for mm-wave heating of reactor relevant plasmae.

Preliminary studies have been pursued with IPP Garching on reactor aspects of Stellarators and on the definition of suitable experiments for this development line.

Detailed progress of the work in the past half year is described in this report. Cooperation with the NET-team, the Joint Research Centres, the Euratom Associations, JAERI and US-laboratories has steadily increased and is gratefully acknowledged.

J.E. Vetter

B 1 Blanket Design Studies

Helium Cooled Ceramic Breeder Blanket

The design studies for the previously described concept of toroidally arranged nearly rectangular canisters filled with a Li_4SiO_4 pebble bed were continued.

An important quantity for this concept is the effective thermal conductivity of the bed. Thus, this quantity was determined experimentally. Fig. 1 shows

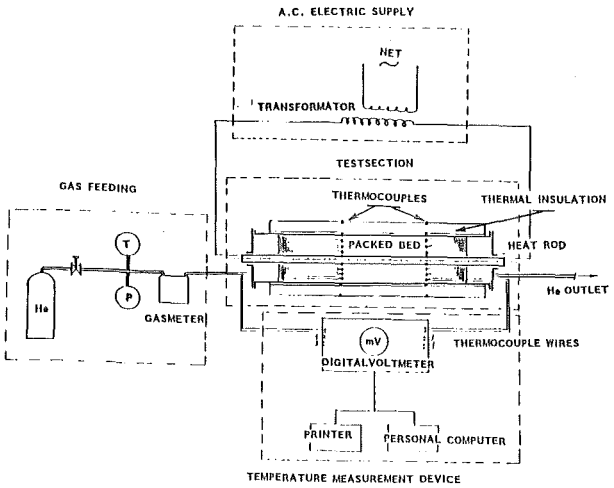

Fig. 1: Facility to measurement the effective heat conductivity of pebble beds.

the arrangement. A 10 cm diameter steel cylinder, electrically heated on its axis, is filled with a pebble bed. Helium through the cylinder and the radial temperature distribution is measured. First results confirm a sophisticated theoretical approach to calculate the effective thermal conductivity of a pebble bed and indicate a value lower than previously assumed. This made a design modification necessary.

Fig. 2 shows a cut through a canister. The plasma facing part of the canister is filled up to 100 mm with rectangular beryllium multiplier bars which are brazed on the helium coolant tubes. There are 6 mm gaps between the bars filled with Li_4SiO_4 pebbles which also form a front layers of about 5 mm thickness. The somewhat complicated shape of this layer (see insert) was necessary to avoid excessive hot spot temperatures. A protective steel coating of the beryllium parts prevents reactions between Li_4SiO_4 and beryllium.

Monte Carlo calculations with a detailed geometrical representation resulted in a tritium breeding ratio (TBR) only one percent below that of a homogenized case. The TBR is high enough to allow for the NET application a blanket only on the outboard side with a shield/reflector component inboard. This is illustrated in the following table:

Configuration		TBR
outboard	inboard	(100% coverage)
blanket	blanket	1.31
blanket	steel He cooled	1.08
blanket	steel H_2O cooled	0.98
blanket	steel He cooled + 2cm Be	1.14

Table 1: Tritium breeding ratio of the Helium cooled canister blanket in NET

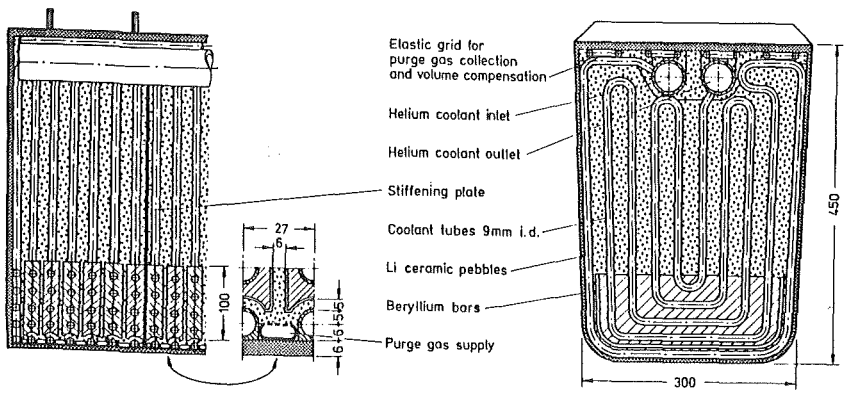

Fig. 2: Canister type breeder blanket element

In collaboration with INTERATOM improvements were made in the assembly of the canisters and cooling tubes. The canisters, together with the intermediate heaters, are fixed to a support structure placed just behind the poloidally running supply tubes. The accomodata thermal expansion the latter are connected with the canisters with long flexible toroidal connection tubes.

Liquid Metal Cooled Blanket

The development of a blanket concept where the eutectic lithium-lead alloy $Li_{17}Pb_{83}$ serves both as breeder material and as coolant has been continued. A feasibility study concluded that the concept is feasible and offers a number of advantages compared to other blanket concepts. The main problem involved in the design of a selfcooled blanket is the influence of the strong magnetic field on the liquid metal flow which causes a high magneto-hydrodynamic (MHD) pressure drop and controls the flow velocity profile. This pressure drop is especially high in the inboard blanket due to the higher magnetic field strength. Therefore an attempt has been made to optimize the tritium breeding ratio of a liquid metal breeder blanket in order to avoid the need for breeding at the inboard side. This led to a new blanket concept which is based on the NET II.2B geometry and is shown in Fig. 3.

The characteristic features of the concept are:

- Breeding blanket at the outboard side only.
- Integrated first wall cooled by liquid metal flowing in toroidal direction similar to the ANL flow concept.
- Arrangement of flow channel inserts in all poloidal flow channels in order to reduce MHD pressure drop and to shape the velocity profile.
- Use of beryllium multiplier in the toroidal channels at the front of the outboard blanket.
- Double containment of the liquid metal by a composite wall.
- Arrangement of a gas cooled steel reflector at the inboard side.

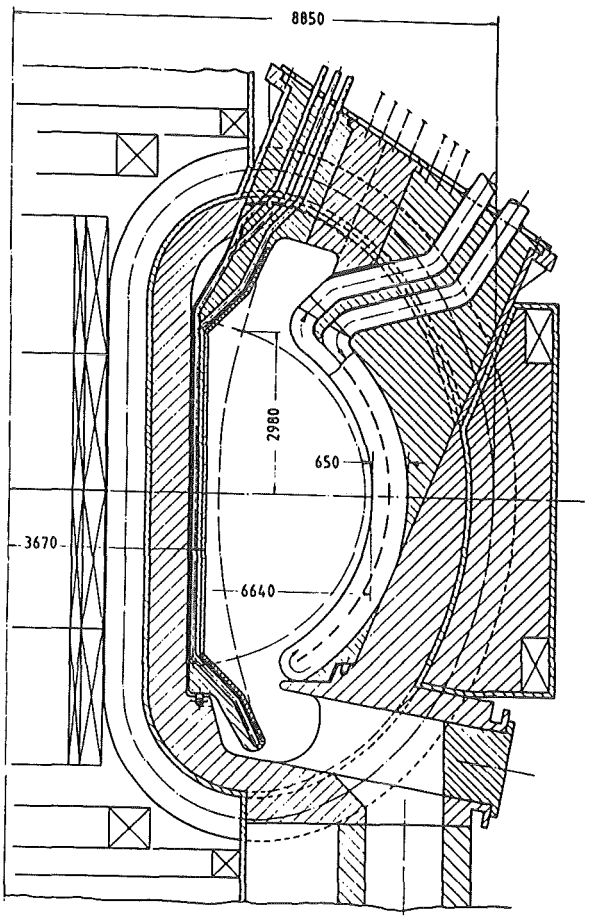

Fig. 3: Liquid metal cooled blanket for NET

- Use of radiatively cooled protection "stones" at the inboard first wall.
- Integration of the divertor plates into the first wall of the inboard segment.

A cross section of the blanket segment is shown in Fig. 4. The height of the toroidal front channel is increased to 100 mm and 75% of the cross section of these channels are filled with the beryllium multiplier.

A total breeding ratio of 1.2 has been calculated for the case of a steel reflector at the inboard side. In this calculation the geometry was approximated by two concentric cylinders for the inboard and outboard segments. A breeding ratio of 1.2 is identical to the value determined for the water cooled liquid metal blanket including inboard breeding. The ratio could be increased to 1.5 if the steel reflector at the inboard side is replaced by beryllium.
Insertion of beryllium in the front channels of the

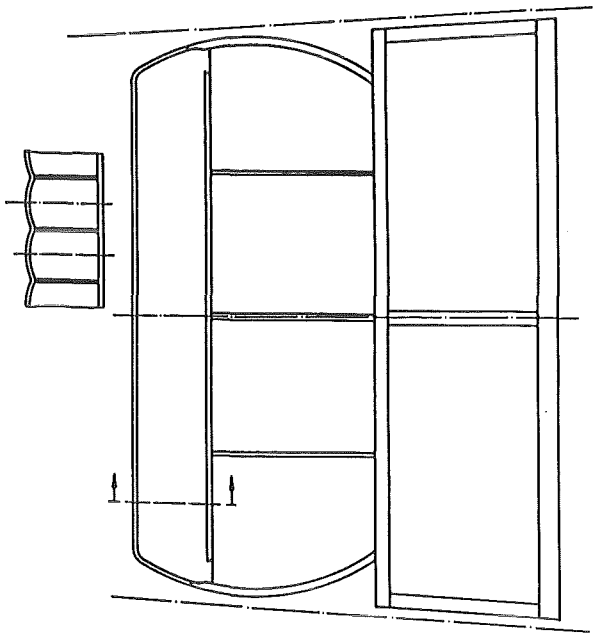

Fig. 4: Blanket cross section

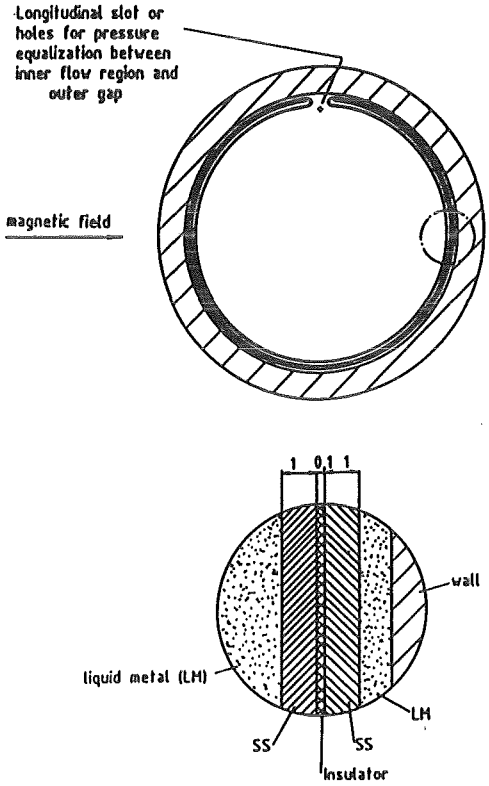

Fig. 5: Flow channel insert

liquid metal cooled blanket has the additional advantage of minimizing the temperature differences in these channels and reducing mechanical stresses in the structural material.

Magnetic forces control the behaviour of the flow, both the velocity profile and the pressure drop. This effect is intensified by the electrical conductivity of the flow channel housing. The dimensioning of the housing is mainly determined by the mechanical load of the structures and can hardly be chosen to achieve a desired velocity profile with a good coolant capability and low pressure drop.

KfK therefore proposes the use of so-called flow channel inserts (FCI) as shown in Fig. 5.

The FCI can be fabricated separately and fit loosely into the channel. All edges of the FCI are sealed by welding, avoiding any contact between liquid metal and insulator. There is no mechanical load on the FCI with the exception of the coolant pressure which, however, is equal on all surfaces. Liquid metal temperature transients cause only small temperature differences across the wall of the insert which can freely expand. Thermal stresses are therefore negligible.

By adequate dimensioning of the thickness of the inner liner of the FCI (maybe different for different side walls in flow channels) it is possible to achieve higher velocity at locations with higher heat input with a minimum of additional pressure drop.

A program has been initiated at KfK to fabricate and test such flow channel inserts.

Alternative Tritium Separation Methods for LiPb-Blankets

For a self-cooled LiPb blanket an intermediate loop is considered advantageous for several safety reasons. If Na or NaK is used in this loop, the following tritium separation method would appear be favourable: the tritium bred in the LiPb permeates through the walls of the intermediate heat exchanger into the Na or NaK and is separated there by cold trapping. The tritium can be recovered by thermal decomposition and stored e.g. in getter beds. An assessment for NET conditions results in a total tritium inventory of only 150 g and acceptable tritium losses to the environment. This technique may be also of interest for a water-cooled LiPb blanket if a tritium purification exists in the water circuit.

Another method studied is tritium permeation with subsequent catalytic oxidation in a gas stream. In this case tritium permeates through a wall material with a high permeability (e.g. zirconium) which is covered on the down stream side with a thin layer of a catalytic material (e.g. palladium). The oxidation at the Pd-surface reduces strongly the tritium partial pressure and causes a relatively small tritium partial pressure in the LiPb. The assessment for NET conditions gave also very favourable results.

Presently, the critical issues of both methods are analysed and required research work is being defined.

Alternative Multipliers

Although lead and beryllium are excellent multipliers from the neutronics point of view there are practical disadvantages with both of them. Lead has a melting point which is low while beryllium is toxic, expensive, and the resources are quite limited. Thus, a lead alloy with a significantly higher melting point than lead could be an alternative. During the STARFIRE study Zr_5Pb_3 has been suggested. However, this material has not yet been fabricated and its properties are unknown.

Therefore, a Zr_5Pb_3 fabrication program was started. After some trials hot isostatic pressing was selected starting with Zr and Pb powders with grains smaller than 90 µ and 30 µ, respectively, pressed at 870°C or one hour at 1500 bar and annealed afterwards at 870°C for 96 hours. First measurements of the Zr_5Pb_3 properties such as density, melting point and thermal diffusivity have been performed. The melting point is higher than 1400°C. A tentative phase diagram based on literature data and similarities to Sn-Zr and Ge-Zr is shown in Fig. 6.

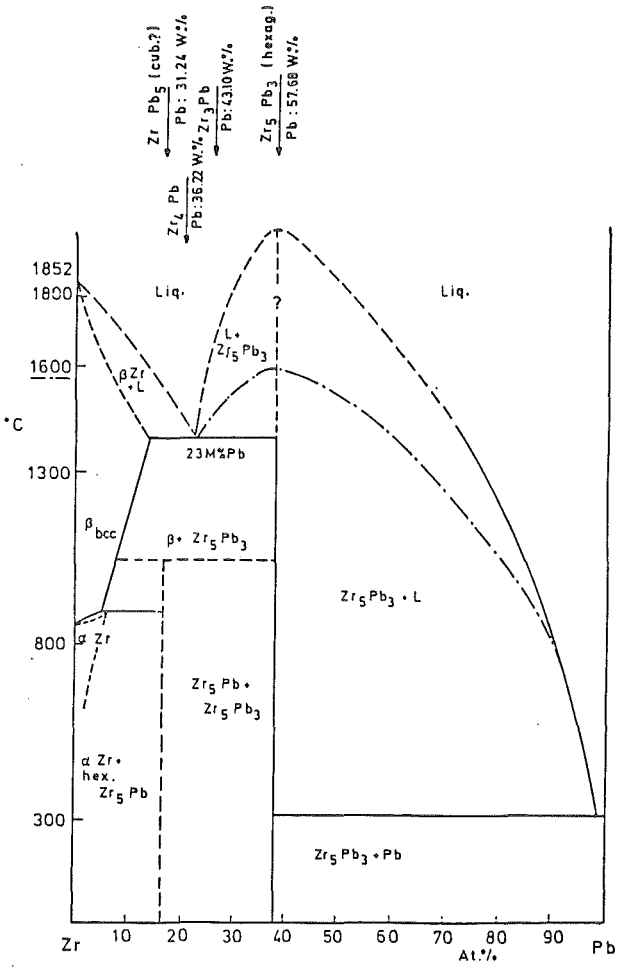

Fig. 6: Phase diagram of Zr_5Pb_3

Staff:

K. Arheidt
E. Bojarsky
V. Casal
M. Dalle Donne
S. Dorner
U. Fischer
B. Haferkamp
M. Küchle
W. Link
S. Malang
P. Norajita
H. Reiser

Publications:

21911
V 21460
V 22265

S. Malang "First Wall Concepts with Radiatively Cooled Tiles", Working Group Meeting on the NET First Wall, Culham, June 18-20, 1985

S. Malang "Flow Channel Insert for the Reduction of MHD Pressure Drop in Liquid Metal Flow", INTOR Phase II a, Third Part, Tokamak Concept Innovations, Vol. II, E.7.4, Vienna, Jan. 1986

M. Dalle Donne, U. Fischer, E. Bojarsky, R. Reiser, "Pebble Bed Canister, A Ceramic Breeder Blanket for high Breeding Ratios", INTOR Phase II A, Third Part, Tokamak Concept Innovations, Vol. II, E.7.5, Vienna, 1986

B 2 Development of Computational Tools for Neutronics

At KfK, a general anisotropic neutron transport system is under development. The one-dimensional module ANTRA1, which had already been set up for plane and spherical geometry, has been extended now to include also the cylindrical geometry option. A new interpolation scheme for determining the angular fluxes, needed for the calculation of the scattering source in the new procedure, had to be introduced. This new interpolation scheme is independent of the actual angular segmentation. At present the cylindrical geometry option of ANTRA1 is tested numerically.

For the generation of the 3-d transfer matrices from double-differential cross-sections (DDX), needed for ANTRA1, a new system of processing codes has been established. This system consists of two major modules: GROUPIE and SDXDDX. GROUPIE, based on the ECN/Petten-code GROUPXS, calculates the 3-d transfer matrices for continuous neutron scattering from DDX-data contained on the European Fusion File (EFF). SDXDDX, which has been developed from the GROUPR-module of NJOY and is implemented as NJOY-module, calculates the 3-d matrices for elastic and level-inelastic neutron scattering from single-differential data (SDX). Both modules use the Legendre representation of the scattering cross-sections in the centre-of-mass system, as it is given on the nuclear data files. But in both modules a transformation scheme has been introduced, which avoids the Legendre-representation in the laboratory system.

At present a first physical test for the DDX-processing code system as for ANTRA1 is performed using the lead nuclear data of EFF-1. This test includes a thorough comparison between full DDX-treatment and conventional P_1-treatment.

The group constant generation code NJOY has the possibility to provide its standard results in different formats. We decided to use the MATXS-format for exchange with external partners. A module JOYFOR was developed, which - via the testing code MITRA - performs the transformation from MATXS-format to the KfK group constant library GRUBA. The code chain NJOY(MATXS) - JOYFOR - MITRA is being extensively tested, e.g. by generating group constants for Li-7 and Be-9 from EFF-1-data using the 171-group structure and the weighting spectrum of the VITAMIN C-library.

The Monte Carlo code MCNP is in use at KfK for the neutronics for fusion blanket design and other purposes. However the MCNP data base available for the European Community is partly very poor. To improve this situation efforts have been made to establish the data preparation code ACER for the actual MCNP version 3 on the IBM computer. First successes were achieved for the cross-sections of Fe56. The CEA Monte Carlo code TRIPOLI, which is also implemented at KfK, promises a better data base. However, for further application, the graphic modules of TRIPOLI are necessary; these are still missing at KfK.

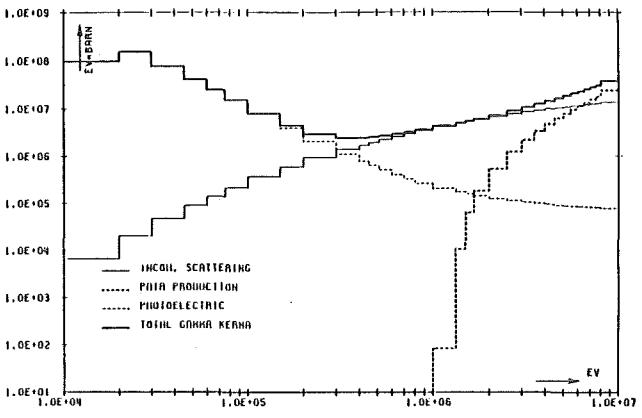

Fig. 7: Total and partial gamma KERMA factors for Zr in 36 gamma groups

Neutron kerma factors for Zr, not available in the VITAMIN-C library, had been calculated previously and were distributed to the European laboratories. Additionally, gamma kerma factors have been calculated now in the 36 gamma group structure of VITAMIN-C. Fig. 7 shows a gamma kerma factors of Zr as calculated from the DLC-7F-data file with NJOY.

Staff:
I. Broeders
U. Fischer
B. Goel
B. Krieg
H. Küsters
A. Schwenk
E. Stein
E. Wiegner

B 6 Corrosion of Structural Materials in Flowing $Li_{17}Pb_{83}$

The corrosion test series of austenitic stainless steel AISI 304 in the pumped LiPb loop was terminated after an accumulated duration of 5500 h. The corrosion effects after 500, 1000, 1500, 4000 and 5500 h exposure time at 420°C are under evaluation. The specimens of cylindrical size - 80 mm diameter - are covered by a layer of the LiPb alloy (∿15 µm thickness). The layer can be removed by means of a treatment in a molten alkali metal (lithium, sodium) or by etching with a mixture of acetic acid and hydrogen peroxide (1:3).

The attack of the liquid metal on the stainless steel specimens is not uniformly distributed. The loss of diameter after 4000 h exposure at 420°C is less than 0.01 mm, local corrosion effects are, however, of the order of 0.01 mm. The local attack seems to be caused by the formation of an alloy of lead with the substitutional elements of the steel (iron, nickel and chromium). Intercrystalline corrosion does not occur under the conditions of our tests. Fig. 8 demonstrates the corrosion resistance of a specimen which has been exposed to the eutectic melt for 4000 h. Under the cover of the adherent LiPb layer there is no evidence for deterioration of the surface layer of the stainless steel.

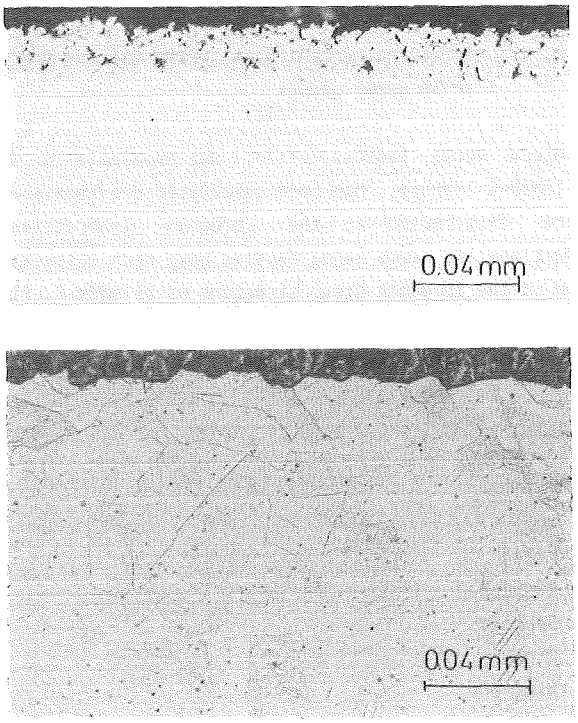

Fig. 8: Cross sections of the surface region of a specimen of stainless steel type AISI 304 corroded 4000 h in LiPb at 420°C in the loop

Staff:

Ch. Adelhelm
H.U. Borgstedt
G. Drechsler
G. Frees
M. Grundmann
Z. Peric

B 9 Tritium Extraction based on the Use of Solid Getters

Several methods were proposed to extract tritium from the liquid Li17Pb83 blanket material. Task B9 will study the use of solid getters. The advantage of this method will be its simplicity and a low tritium inventory in the blanket, while most of the tritium is always fixed in the getter.

For the studies the loop TRITEX is under construction and scheduled for early 1987. It will be a pumped Li17Pb83 loop, permanently adding hydrogen (D_2, H_2, HT) to the circulating metal.

In the laboratory the studies continued, using samples of Li17Pb83 of about 30 to 50 g in crucibles of Al_2O_3 and molybdenum. To find the reasons for losses of lithium from the samples, the oxidation in air and the evaporation in vacuum and under argon were investigated.

No protective oxide layers were formed in air, the oxidation followed always a zero order reaction kinetics. Weight gains after 24 hours as a function of the reziprocal temperature are shown in Fig. 9. The activation energy for the oxidation of the solid alloy was found to be 6.4 kJ/mol, and for the molten alloy to be 60 kJ/mol.

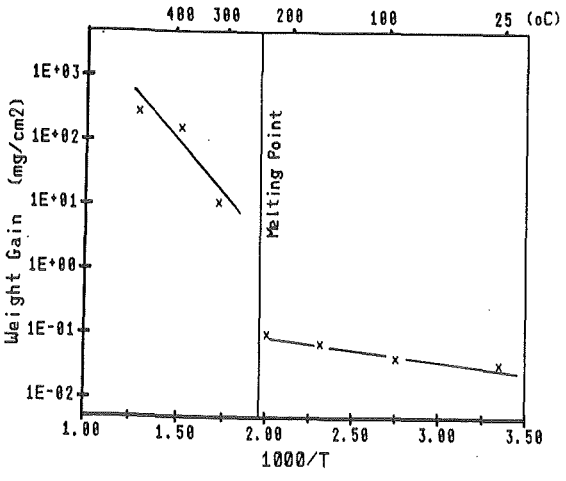

Fig. 9: Oxidation rate of Li17Pb83 in air.
Values given for 24 hours oxidation.

The oxides formed extract lithium from the alloy. About 50% of the lithium is found in the oxides after oxidizing 1% of the metal, and more than 99% is shifted to the oxides after the reaction of 2% of the metal. The formed oxide layers contain stable Li-compounds, which cannot be reduced by stagnant hydrogen at 800°C.

Evaporation of the alloy removes lithium, too. Fig. 10 shows evaporation rates, obtained at a pressure below 1 mPa. The activation energy was found to be 158 kJ/mol for the temperature range between 400 and 600°C.

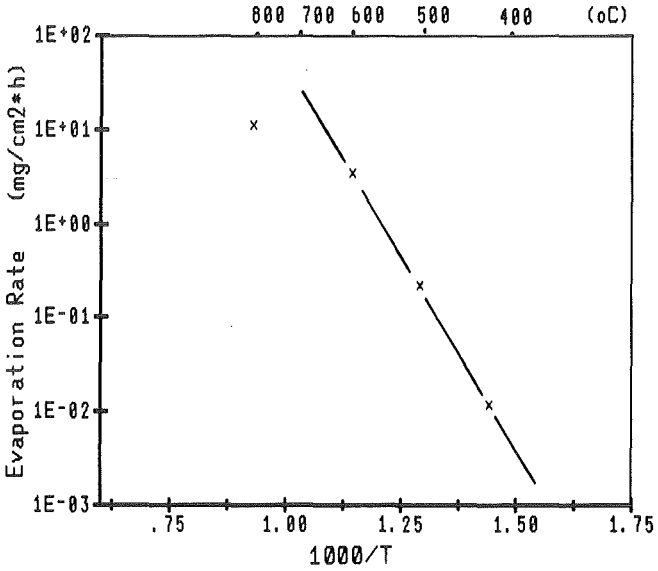

Fig. 10: Evaporation rate of Li17Pb83 under vacuum

Evaporation rates are high at higher temperatures. In this case also the evaporation of lithium is high. Under the conditions of the experiments at 800°C, 20% of the lithium evaporated together with only 0.2% of the sample within 2.8 hours, and 30% of the lithium together with only 1% of the sample within 15 hours.

Evaporation of the lithium lead alloy under argon of one bar is much lower. At 725°C, for example, the evaporation rate was 0.7 $mg/cm^2 \cdot h$, which is still a considerable evaporation rate.

Summarizing, it can be concluded, that oxidation as well as evaporation of Li17Pb83 removes lithium from the alloy. These effects are probably, responsible for reduced lithium concentrations often found. Furthermore it was demonstrated, that lithium moves also into ceramic crucible material; this effect has to be taken into account also when discussing lithium values.

Staff:

H. Feuerstein H. Gräbner

B 11-16 Development of Ceramic Breeder Materials

1. Preparation of Li_2SiO_3 and Li_4SiO_4 Pellets

The preparation and fabrication of lithium containing monosilicates, especially Li_2SiO_3 and Li_4SiO_4, are under development to be used as breeder materials for fusion reactors within the European Fusion Program (Tasks B 11 and B 12). The monosilicate powders are normally sintered to pellets or disks with a cylindrical shape, a geometry, which is especially suited for irradiation tests and basic material studies. Due to the particular blanket design which is under development at KfK (see also B 1) small spheres or nearly spherical particles with diameters in the range of 0.5 to 1.0 mm are of special interest within this program. First experiments have been carried out for the preparation of such materials which shall lateron be scaled-up to industrial production.

A number of Li_2SiO_3 and Li_4SiO_4 pellets were prepared to obtain information on the physico-chemical properties as well as on the irradiation behaviour, based on the preparation method already described in detail. The samples were especially prepared for irradiation tests at Saclay (OSIRIS-reactor, DELICE-02) and at KfK (KNK II-reactor, ELIMA-01). The monosilicate pellets were characterized metallographically, and by X-ray diffraction analysis, mercury intrusion porosimetry, scanning electron microscopy, gas permeation measurement, as well as chemical analysis. Special informations on the samples prepared are given in table 2.

2. Preparation of Spheres and Spheroidized Materials

Li_4SiO_4 spheres with diameters of up to 4 mm were prepared from sintered cylindrical pellets by grinding methods. The deviation from the spherical shape was only in the range of 10 to 20 µm. This rather expensive technique may only be suited for special experiments. Li_4SiO_4 spheres were fabricated by this technique for an international irradiation experiment at JAERI, Japan (JRR-2 reactor, BEATRIX-program).

Experiments to prepare ball-shaped particles by normal agglomeration techniques were not successful due to the gliding properties of the spray-dried silicate powders. Sufficient results were obtained by extruding the wetted monosilicate powders with subsequently rounding on a special rotating disk ("Extruder" and "Spheronizer" from NICA-SYSTEMS). Nearly spherical monosilicate particles with diameters of about 1 mm resulted after sintering. The surface of the particles is smooth and their density has been measured to be in the range of 80 to 90% th.d. It is foreseen to prepare larger batches of this material to watch the fluidizing and gliding properties under mechanical stress conditions. The advantage of this preparation method is given by the possibility in scaling-up this method to a industrial fabrication.

The samples necessary for in- and out-of-pile measurements were fabricated and characterized according to the specifications given in table 2. It has been shown that nearly spherical monosilicate particles can be fabricated by a special technique based on extruding and pelletizing of wetted silicate powders. Further work is needed to optimize this technique and to improve the spherical shape of the particles.

experiment	material	density (% th.d.)	shape	diameter (mm)	number of samples	remarks
DELICE-02	Li_2SiO_3	65	pellets	5	60	irradiation test, OSIRIS
		90	pellets	5	60	
	Li_4SiO_4	65	pellets	5	110	
		90	pellets	5	110	
ELIMA-01	Li_2SiO_3	65	pellets	5	50	irradiation test, KNK II
		65	disks	5	50	
		90	pellets	5	50	
		90	disks	5	50	
	Li_4SiO_4	65	pellets	5	50	
		65	disks	5	50	
		90	pellets	5	50	
		90	disks	5	50	
VOM 23 H	Li_4SiO_4	90	spheres	4	500	irradiation test, JRR-2
IMF I	Li_2SiO_3	90	disks	8.5	110	Be-compatibility,
INR	Li_4SiO_4		powder		4 kg	experiments with melts.
IMF III	Li_2SiO_3	42	pellets	16	15	green pel.,
		75	pellets	9.5	15	sint. pel., HIP-exp.

Table 2: Prepared Samples of Li_2SiO_3 and Li_4SiO_4

Publication:

D. Vollath, H. Wedemeyer, "Preparation of the lithium silicates series from Li_2SiO_3 to Li_8SiO_6 in alcoholic media", Second Int. Conf. Fusion Reactor Materials (ICFRM-2), April 13-17, 1986, Chicago

Staff:
B. Dörzapf
H. Elbel
E. Günther
R. Hanselmann
J. Heger
W. Jahraus
E. Kaiser
W. Laub
N. Nagel
R. Scherwinsky
D. Vollath
H. Wedemeyer
M. Wittmann

3. Measurement of Physical, Mechanical and Chemical Properties of Ceramic Breeder Materials (B 13)

Constitution and Thermodynamics

The phase relations in the Lithia-rich part of the Li_2O-SiO_2 system have been investigated by thermal X-ray diffraction analyses. Particular experimental methods were applied to obtain equilibrium conditions. Sample preparation was performed under dry and inert atmosphere, starting materials were Li_2O and SiO_2 powders, and thermal treatment of the samples was carried out in sealed capsules to prevent loss of Li_2O by evaporation. The lithia-rich compound Li_8SiO_6 was found to be thermodynamically stable at temperatures up to 830°C. At higher temperatures it dissociates into Li_2O and Li_4SiO_4, melting occurs close to 1000°C. The melting temperatures are increased with decreasing Li_2O content due to evaporation losses. Up to now, no other stable compounds have been found in this part of the Li_2-SiO_2 system, but the investigation is still continuing. The lattice parameters of the hexagonal phase Li_8SiO_6 (space group $P6_3$ cm) prepared as described above are:

$$a_o = 542.8 \text{ pm}; \quad c_o = 1063 \text{ pm}$$

resulting in a theoretical density of 2.2 g/cm^3 and a theoretical lithium atom density of 0.68 g/cm^3.

The interaction of Li_3SiO_4 with water vapour was investigated from room temperature up to ∿ 800°C by thermoanalytical methods (esp. thermal microbalance, partly combined with DTA). In the whole temperature interval and at water vapour concentration up to 27000 ppm no evidence was found for the formation of LiOH in the condensed phase. In the low temperature region up to ∿ 300°C only adsorption and desorption of water is observed. Above ∿ 300°C moisture provokes mass losses, probably due to evaporation. The mechanism is not quite understood as yet.

Physical and Mechanical Properties

As the measured values of C_p for λ-$LiAlO_2$, published in the literature, /1,2/ differ widely the specific heat of this compound was measured in cooperation with the University of Stuttgart. The differential scanning calorimeter of Perkin-Elmer was used. The calibration was performed with a NBS-Sapphire as reference material. Samples prepared via Li_2CO_3 and via $Li\,Al_2(OH)_7$ were used. Both data sets confirm the values of Christensen /1/ and follow the equation:

$$C_p = (1.372_5 + 2.278_0 \times 10^{-4} \cdot T - 39405/T^2) \text{ J/gK}$$

$$300 \leq T \leq 1000 \text{ K}$$

The thermal diffusivity α_0 of 100% dense λ-$LiAlO_2$ prepared via $Li\,Al_2(OH)_7$ was determined from experimental data on samples of various porosities ($10 < p < 22\%$). The diffusivity follows the equation:

$$\alpha_0 = 8.185 \times 10^{-2} - 2.0545 \times 10^{-4} \cdot T + 2.0075 \times 10^{-7} \cdot T^2 - 6.6188 \times 10^{11} \cdot T^3) \text{cm}^2/\text{sec}$$

$300 \leq T \leq 1275$ K, $r = 0.9998$, r = coefficient of regression.

For samples with completely open porosity p the following corrections have to be made:

$$\alpha_p = f(p)\alpha_0 \qquad f(p)\left[= \frac{4 - 9p}{10(1-p)} + \sqrt{\left(\frac{4 - 9p}{10(1-p)}\right)^2 + \frac{1}{5}}\right]$$

For samples with 12.3 % porosity f(p) equals 0.889. For comparison, we measured the thermal diffusivity of a 12.3 % porous γ-$LiAlO_2$ prepared via Li_2CO_3. In the temperature region 373 K < T < 1000 K the data confirmed once more the above mentioned porosity correction for open porosity. The calculated data are within the margin of error of the measured values for 12.3 % porous samples.

The thermal shock resistance was determined on Li_2SiO_3 and $LiAlO_2$ pellets. It is defined as the lowest temperature difference ($\Delta T_{critical}$) at which under

given boundary conditions cracking occurs. The pellets were thermally shocked by dipping into liquid tin of higher temperature. The Li_2SiO_3 pellets (9.4 mm diameter, 9 mm height) had been manufactured at KfK/IMF III, the $LiAlO_2$ pellets (9.8 mm diameter, 10 mm height) by CEA. The results are shown in Table 3. The critical temperature differences are higher for

	Li_2SiO_3		$LiAlO_2$	
Density, % TD	92	82	88,5	73
$\Delta T_{critical}$, K	790	700	440	490
Thermal shock resistance parameters for 90% TD				
$R' = \frac{\sigma(1-\nu)}{\alpha E} k$, $\frac{W}{cm}$	3		5	
$R''' = \frac{E}{\sigma^2(1-\nu)}$, $\frac{cm^2}{N}$	15		10	
Young's modulus E, GPa	80		95	
Poisson's ratio ν	0.23		0.23	
compr. strength σ_c, MPa	420		550	
tensile strength σ, MPa ($\sigma \hat{=} \sigma_c/5$)	84		110	
thermal expansion α, 10^{-6}/K	13.4		12.6	
thermal conductivity k, W/cm K	0.05		0.07	

Table 3: Thermal shock behaviour of Li_2SiO_3 and $LiAlO_2$

the silicate than for the aluminate. To interpret these results the thermal shock resistance parameters R' and R" were calculated. R', which describes the resistance to crack initiation, is higher for the aluminate, whereas R''', which characterizes the resistance to crack propagation, is higher for the silicate.

Compressive creep tests on Li_2SiO_3 specimens of different porosity (8-12%) resulted in creep rates between $2x10^{-5}$ and $3x10^{-4}$/h at 40 MPa and 900°C.

References

/1/ A.O. Cristensen, K.C. Conway, K.K. Kelley, US-Bureau of mines RI-5711 (1960) (quoted after /2/)

/2/ G.W. Hollenberg, D.E. Baker, Report HEDL-SA-2674-FD (1982)

The Solubility of Hydrogen in Solid Breeding Materials

Whereas a compilation of numerical data of thermophysical, thermochemical and mechanical properties of ceramic breeder materials is now available from different laboratories, nearly no data exists to the solubility of hydrogen isotopes in candidate lithium ceramics. In order to measure the solubility, a gas volumetric apparatus has been built and is now completely equipped for experiments with tritium. In Fig. 11 the glove box on the right is designed for handling of the lithium ceramic samples under a very dry argon atmosphere $P_{H_2O}/P_{tot} \lesssim 1$ppm) and the one on the left contains the equipment for the solubility measurements.

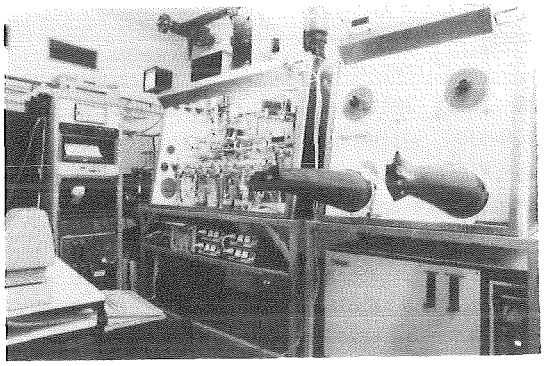

Fig. 11: View to the apparatus for solubility measurements of hydrogen isotopes in lithium ceramics

In order to demonstrate the feasilibity of the experiments and to calibrate the apparatus, nickel samples are used. The results of these calibration runs, carried out at 500°C, are shown in Fig. 12. It is seen that the obtained results correlate with an extrapolation of the experiments from McLellan and Oates from 1973.

Presently the solubility of light hydrogen in Li_2SiO_3 is under investigation at 450°C. Approximately 800 tablets (46 g) pressed from silicate powder have been stacked inside the sample vessel. The ratio of the sample volume V_s to dead space volume V_d was found to be 0.4. Therefore solubilities greater than a few times 10^{-6} give a Δp of 1 mbar (see Fig. 13) and may adequately be detected.

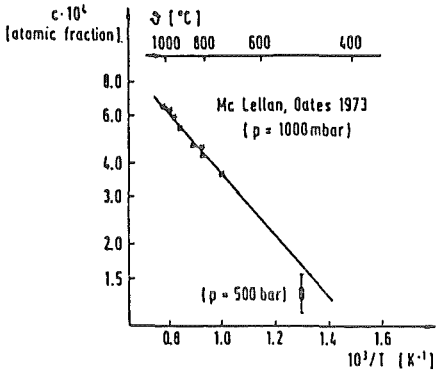

Fig. 12: Solubility of light hydrogen in nickel; comparison of measured with literature values

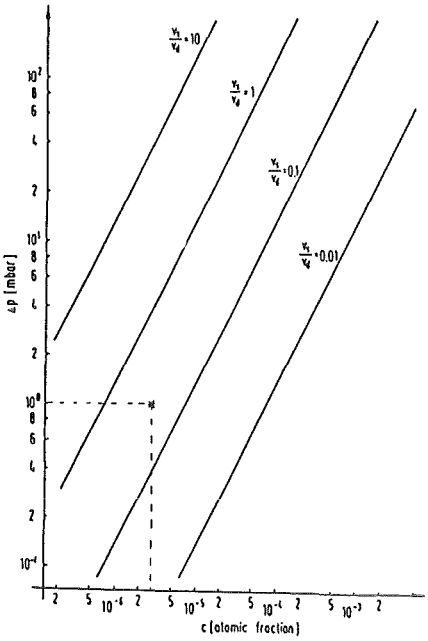

Fig. 13: Expected pressure signal as a function of hydrogen solubility in Li_2SiO_3; parameter is the ratio of sample volume to dead space volume

First results support previous measurements carried out at high hydrogen pressure (60 bars), which indicated that the solubility is very low.

Staff:
M. Glugla
R.D. Penzhorn
K.H. Simon

4. Compatibility with Stainless Steels (B 14)

The 600, 700 and 800°C annealing tests with Li_2O, Li_2SiO_2, Li_2SiO_3 and Li_4SiO_4 powders pressed into capsules of SS 316 and 1.4914 (11% Cr, martensitic-ferritic) were finally evaluated. There was no major difference in the cladding attack produced with H_2O or NiO additions. Fig. 14 shows the reaction rates including the results of the two cladding materials with both oxidants each. It seems that technically considerable cladding attack has to be expected above about 700°C with Li_2O, 800°C with Li_4SiO_4, and 900°C with Li_2SiO_3.

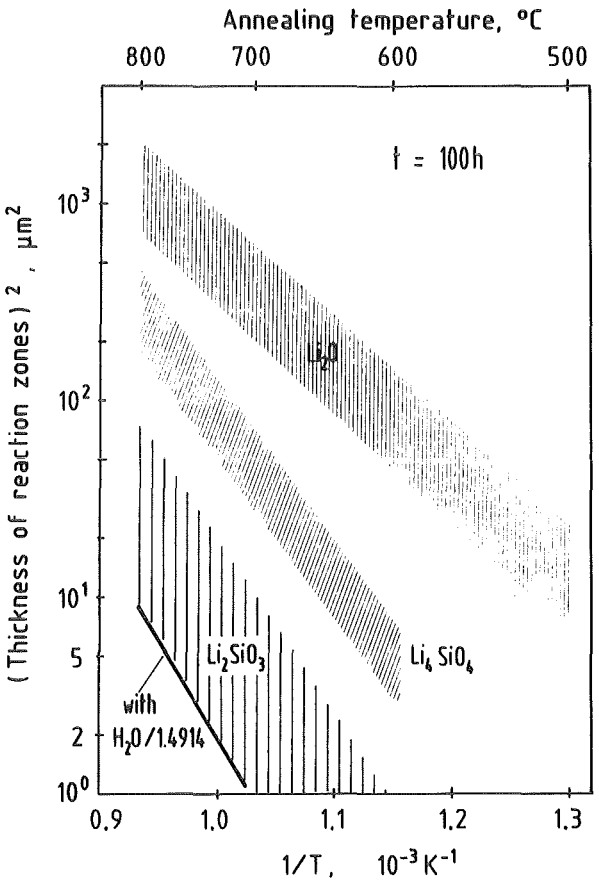

Fig. 14: Chemical attack of oxide breeder materials with 1 mol % H_2O or NiO) on stainless steel

Staff:
Ch. Adelhelm
M. Blumhofer
W. Dienst
G. Haase
P. Hofmann
K.-H. Kurz
H. Metzger
V. Schauer
G. Schlickeiser
B. Schulz
A. Skokan
H. Strömann
H. Zimmermann

5. Irradiation Testing of Ceramic Breeder Materials (B 15)

After finishing a first irradiation DELICE 01 of 45 KfK lithium metasilicate sample columns in the OSIRIS reactor at Saclay, the dismantling and the post irradiation examinations will begin in April 1986. The facilities for tritium release measurements are already installed and tested in the Karlsruhe hot cells. The second experiment, DELICE 02, has started with 20 sample columns of Li_2SiO_3 and Li_4SiO_4 by end of March 1986. Two further irradiations DELICE 03/04 are foreseen for irradiation in 1987.

A first irradiation ELIMA 01 is presently under preparation for insertion into a material test rig in the fast reactor KNK II at KfK. The main objective is to achieve higher neutron damage due to the fast flux and to have exactly controlled and determined temperature conditions. In order to meet the desired temperature ranges of 400-450°C and 650-700°C, respectively, the samples shall be irradiated in two different capsule variants: for the low temperature range a sample carrier is provided, in which up to 26 sample columns with SS cladding are directly rinsed by the soium of the reactor coolant (Fig. 15). In the high temperature device, up to 28 samples are mounted in a double-walled capsule with insulating gas gap. This gap together with a gas-buffered heat pipe allows to adjust quite exactly the esired temperature for the samples and makes it possible to hold the temperature constant also at varying power, (Fig. 16).

For the experiment ELIMA 02, which is planned for early 1987, it is intended to have a specimen matrix identical to the experiment DELICE 03 (also identical samples, see Fig. 17) in the thermal reactor OSIRIS in order to get close comparison of the influence of different neutron spectra.

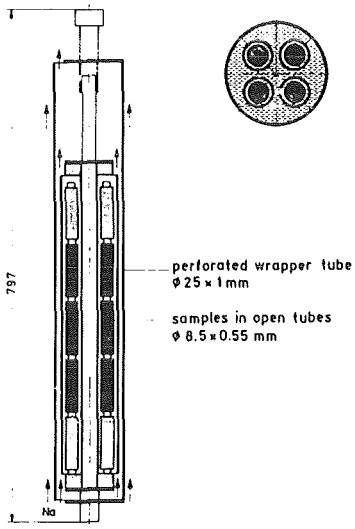

Fig. 15: KNK sample carrier for temperature range 400 - 450°C

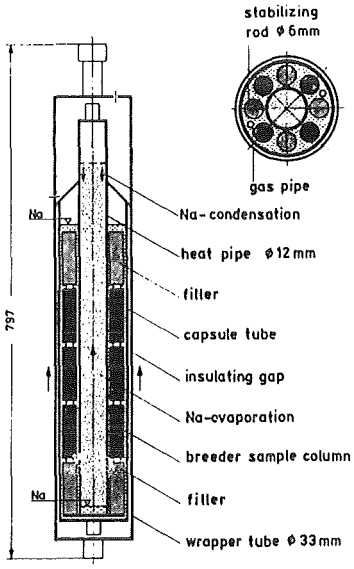

Fig. 16: KNK sample carrier with heat pipe for temperature range 650 - 700°C

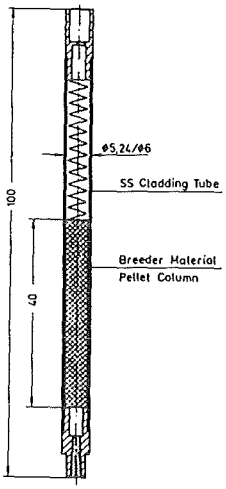

Fig. 17: Breeder material sample rod for irradiation in KNK and OSIRIS

Staff:

E. Bojarsky
H. Elbel
H.E. Häfner
H. Werle

6. Tritium Recovery from Ceramic Breeder Materials (B 16)

The LISA1 experiment is a test of in-situ tritium release. Conducted in the SILOE reactor at CEN Grenoble, the experiment uses the same facilities as LILA1. The experiment has six capsules, four with Li_2SiO_3, one with Li_4SiO_4 and one with $LiAlO_2$. Each capsule is separately purged. The tritium activity is determined by ionization chambers and scintillation counting. An important difference as compared to LILA1 is the use of zinc beds to reduce tritiated water and thereby prevent sorption of T_2O on the lines. Irradiation began on October 25, 1985 and was continued for three 3-week-cycles. The testing included systematic variation of four parameters: temperature (450 to 730°C), neutron flux (0.8 to 2.7 x 10^{13} $1/cm^2 \cdot s$), sweep gas flow rate (1.8 to 7.0 L/h), and sweep gas composition (He, He + 0.1% H_2, He + 0.2% O_2). A condensed test matrix is given in Tab. 4.

The results of first, preliminary evaluations are:

System:
- Measured T-activities seem reliable (ionization chamber and scintillation data agree)
- Results are reproducible
- Zn-reductors work efficiently (only small amount of T on lines)
- Steady state achieved in most runs (release independent of time and temperature for higher temperatures, release equal production)
- Addition of H_2 reduces permeation.

Samples:
- Addition of O_2 is detrimental to release
- Fraction of T_2O (of total T species) formed in the He purge gas:
  Li_2SiO_3/Li_4SiO_4: 15 %
  $LiAlO_2$: 50 %
- Types of inventory

	He	He+0.1%H_2
Aluminate	Mainly diffusion	
Orthosilicate	diff.+other (surface?, diff.)	diff.
Metasilicate	diff.+other	("trapping"?, diff.)

- Addition of H_2 improves release for orthosilicate and aluminate. The behaviour is diffusion-like, the inventories are very small (see Table 5).

Some important preliminary conclusions are:

- Zn-reductor is necessary for T-transport from samples to the monitors.
- Systematic variations of the neutron flux were done the first time in inpile tests and were found to be very valuable for determination of T-inventory.
- Similar samples in the same test avoid overinterpretation, different samples in the same test allow reliable comparison.

- The behavior of orthosilicate with He+0.1% H_2 is diffusion-like, the inventory is very small, even at low temperatures.

The next inpile test, LISA2, is planned for the end of this year.

Publication:

H. Werle, J.J. Abassin, M. Briec, R.G. Clemmer, H. Elbel, H.E. Häfner, M. Masson, P. Sciers, H. Wedemeyer, "The LISA1 Experiment: In-Situ Tritium Release Investigations", Second Int. Conf. Fusion Reactor Materials (ICFRM-2), April 13-17, 1986, Chicago

Staff:

R.G. Clemmer
H. Elbel
H.E. Häfner
H. Wedemeyer
H. Werle

Cycle	Date	Run	Purge gas Type	Flow F	Neutron flux ϕ	Sample temp. T	Purpose
A	Oct.25-Nov.14, 85	1-7	He	1.0	~1.0	T T-50 T-100	Verify steady state Inventory I(T)
		8	He+0.1%H_2	1.0	~1.0	T	Purge gas chemistry
B	Nov.28-Dec.19, 85	1-10	He+0.1%H_2	1.0 1.7 0.7	1.0 1.7 0.8	T T-100 T-150	Verify steady state I(T,ϕ,F) Permeation
C	Jan.11-31, 86	1-10	He+0.1%H_2	1.0 1.7 2.5	1.0 1.7	T T-50 T-130	Verify steady state I(T,ϕ,F) Permeation
		11-13	He	1.0 2.5	1.0 1.8	T	Purge gas chemistry I(ϕ,F), Permeation
		14	He+0.2%O_2	1.0	1.0	T	Purge gas chemistry
		16	He	1.0	1.0	T	Shutdown Zn-reductor+T_2/T_2O

Reference values Flow F 2.5 L/h (actual conditions)
Flux ϕ $1.3 \cdot 10^{13}$ $1/cm^2$ s
Temperature T, upper plane (P1, P3, P6) 700 °C
lower plane (P2, P4, P6) 600 °C

Table 4: Condensed test matrix

Temp. (°C)	P6, Orthosilicate, p=4.76 mC/h I(mc)	τ(h)	D(cm^2/s) r=13μ	r=.4cm	P2, Aluminate, p=4.80 mC/h I(mc)	τ(h)	D(cm^2/s) r=.19μ
450	50.8	10.7	-	-	-	-	-
500	22.3	4.7	$0.7 \cdot 10^{-11}$	$0.7 \cdot 10^{-6}$	41.9	8.7	$0.8 \cdot 10^{-15}$
550	8.6	1.8	$1.7 \cdot 10^{-11}$	$1.7 \cdot 10^{-6}$	11.3	2.4	$2.8 \cdot 10^{-15}$
600	5.7	1.2	$1.6 \cdot 10^{-11}$	$2.6 \cdot 10^{-6}$	3.6	0.8	$8.3 \cdot 10^{-15}$
630	5.1	1.1	$2.8 \cdot 10^{-11}$	$2.8 \cdot 10^{-6}$	2.7	0.6	$11 \cdot 10^{-15}$

p = production rate, I = inventory
τ = I/p residence time, D = $r^2/15\ \tau$ diffusion coefficient,
r = characteristic radius for diffusion

Table 5: Diffusion inventories, purge gas He+0.1% H_2

M 1 The Large Coil Task (LCT)

The project has entered an important phase. A target date was fixed by the Project Officers and the Executive Committee to finish the installation work in the IFSMTF (International Fusion Superconducting Magnet Test Facility). All components should be installed and ready for the Six Coil Test till October 24, 1985. The lid could go on the large vacuum vessel with all components installed (6 LCT coils and the pulse coil system) as scheduled (Fig. 18).

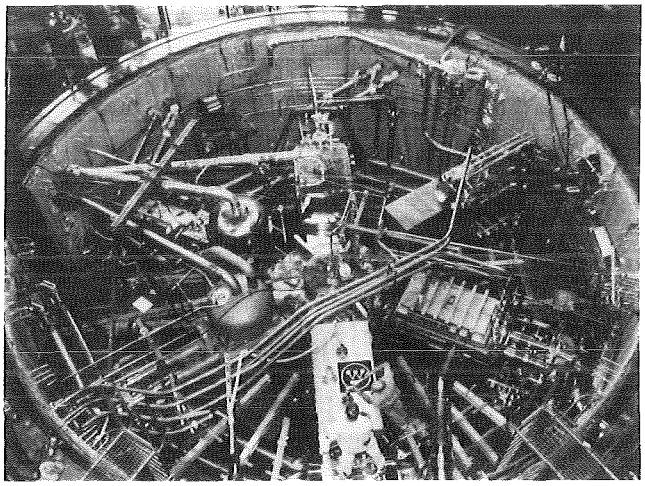

Fig. 18: The vacuum vessel with the torus of six superconducting LCT coils and the pulse system, for the simulation of poloidal fields transients

Pumping down four times and returning to atmospheric pressure, as well as a two times removing the lid, were necessary to fix air and helium leaks. Three helium leaks were found and localized. Two of them, the leaks on the Swiss (CH)-coil and the General Electric (GE)-coil could be repaired, one of them, the leak on the General Dynamics (GD) coil was within acceptable limits. A total leak rate of 2×10^{-4} mbar l/s was measured before cooldown, thereby the GD-coil leak with 1.4×10^{-4} mbar l/s was the biggest contribution. Measuring of leak rates and localization of leaks were performed with a leading role by a KfK staff member. After repairing some water leaks in the oil cooler of the helium compressors and fixing the fast front ends of the data aquisition, cooldown could be started on December 18, 1985. A leak in the liquid Nitrogen cooldown heat exchanger forced to an interruption of the cooldown. In a remarkable short time the heat exchanger could be replaced by one taken from a refrigerator of the same type presently not in use at the Lawrence Berkeley Laboratory. On January 18, 1986 cooldown was restarted and after about 680 hours cooling of the 400 t facility the Westinghouse coil with its Nb_3Sn conductor became superconducting (Fig. 19) first. The NbTi coils entered in the

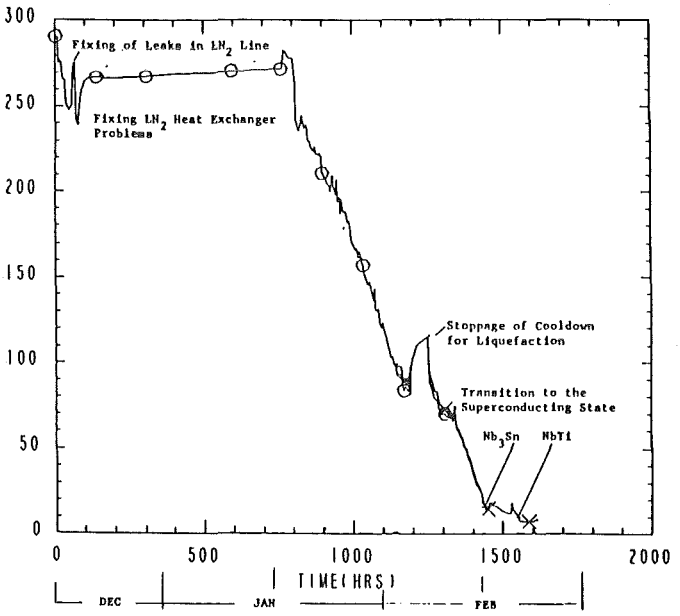

Fig. 19: History of cooldown of the IFSMTF demonstrated by the inlet temperature of the Euratom LCT coil.

superconducting state about 110 hours later on February 18, 1986. The results of the cooldown can be summarized as follows:

- The Euratom LCT coil showed excellent heat transfer properties. Its average temperature was always 5 K below the other coils.

- The cooldown rate of about 0.4 K/hour allowed a good equalization of temperatures as well in the coils as in the structure of the facility.

- The pulse coil system with relatively poor thermal coupling to parts of the structure, was actively cooled two times by its LN_2-circuit to bring it down to about 100 K.

- The leak rate at 4.2 K increased to about 0.1 mbar l/s but it could successfully be handled by the available pumping power. No further leak source was identified.

After reaching superconductivity in all coils, a

period of intensive checkouts (high voltage insulation tests, balancing of the quench detection systems, instrumentation) was started.

- All coils pathed their high voltage test within acceptable limits, with exception of the GD coil which still shows a breakdown to ground between 400 V to 600 V.

- The Euratom quench detection system showed a good compensation of the inductive voltages but also a slight dependence on the ramp rate of the pulse generator.

During this period, one of the compressors failed and had to be exchanged. Operation with 3 and 2 compressors was practiced without disturbance of the running checkouts and the filling up to the coils with He. The forced flow cooled coils were hold in a stand by mode at about 5.7 K.

Single coil tests were started in the sequence JA, CH, GD/C, GE, EU, WH, as agreed in September 1985 by the Project Officers.

After initial checkouts the Japanese coil run successfully through the complete single coil test programme:

- Dump tests up to 60% of rated current,
- ramping up to full rated current,
- stability tests up to full rated current,
- nuclear heating test combined with stability test up to 90% of rated current,
- and finally rechecking by ramping up again to full current.

During dump tests the induced currents in the other 6 coils were measured and compared with calculation models. Steady state heat load measurements with the vapour cooled current lead dewars filled, resulted in a load of 66 - 80 W for each coil. Therefore a total heat load of about 500 W, including the structure, can be expected from the torus. It has to be taken into account that about one half of the heat load appears at 4.2 K temperature level and the other half at 3.8 K. The losses of the vapour cooled leads for the Japanese coil at rated coil current were measured to 48 l/h for one lead and about 44% higher for the other lead. Further analysis will be carried out to reach an improvement in lead losses.

The test of the Japanese coil was finished on March 24, 1986. 9 working days with 14.5 hours/day were needed, thereby the coil was 29 hours under current. At the end of the reporting period checkout are running for the start of the single coil test of the Swiss coil.

KfK/Euratom participates since November 1985 with 4 staff members in all the preparatory work and these tests.

Staff:
G. Friesinger
W. Herz
H. Katheder
P. Komarek
G. Nöther
L. Siewerdt
M. Süßer
A. Ulbricht
F. Wüchner
G. Zahn

M 3 Development of High Field Composite Superconductors

1. Investigations on Subzize NET Model Conductors

A detailed study on a NET relevant subsize Nb_3Sn conductor has been undertaken. The subscale conductor (external dimension of 5 x 12 mm^2) consists of a flat Nb_3Sn cable soldered into a Cu stabilizing structure which is in turn contained in an external steel case. The variation of the critical current I_c, of the subsize conductor with applied strain ε was measured at 12 T in a new 10 kN test rig. A task of particular interest consisted in testing I_c vs. ε separately for each constituent, a) the Nb_3Sn multifilamentary wire, b) the flat Nb_3Sn cable made with this wire, c) Nb_3Sn cable with the soldered Cu stabilizing structure and finally d) the complete conductor.

For this purpose, different strain rigs, one for 1 kN/200 A, the other for 5 kN/150 A, taking into account the different cross-sections, were used.

The characteristics of the conductor (Fig. 20) are as follows: The Nb_3Sn wire of Ø 0.39 mm consists of 4500 filaments of Ø 3 µm in a bronze matrix, with a twist pitch of 50 mm. The flat cable is composed of 7 Nb_3Sn wires and 5 stabilizing Cu/Ta/Cu wires of the same diameter twisted around a Duratherm ribbon resulting in 0.5 x 2.5 mm^2 cross-section. After reacting 64 hours at 700°C, the flat cable is soldered into the Cu stabilizer and inserted in two U-shaped steel profiles which are joined together by continuous laser welding. This welding process has a high energy density, leading to low heat input, thus maintaining the temperature below the melting point of the solder (≈ 200°C).

The results of I_c vs. ε at 12 T on each constituent of the subsize conductor are represented in Fig. 21. It is seen that all cases exhibit the well-known maximum of I_c at a strain ε_m. The value of ε_m increases from ∿0.2% for the Nb_3Sn wire to ∿0.3% for the cable, to 0.4% for the cable soldered in Cu and finally, ≥ 0.5% for the assembled conductor (the last value can only be estimated, the force of 10 kN being insufficient for 60 mm^2 cross section). Two points in Fig. 21 are of particular interest: a) the horizontal portion for the flat cable reflects the initial alignment of the Nb_3Sn wires around the Duratherm core. A tensile stress on these wires occurs only at the end of the horizontal portion, ε_m being

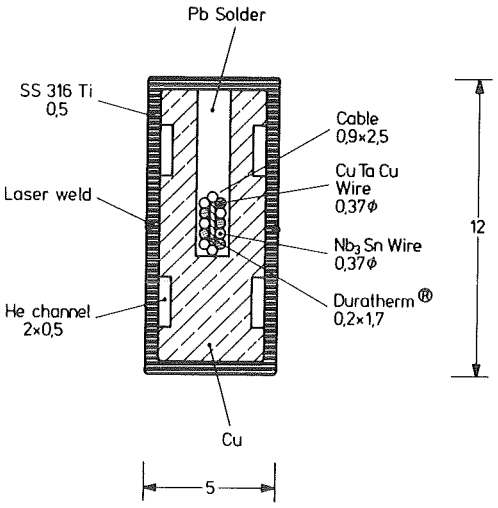

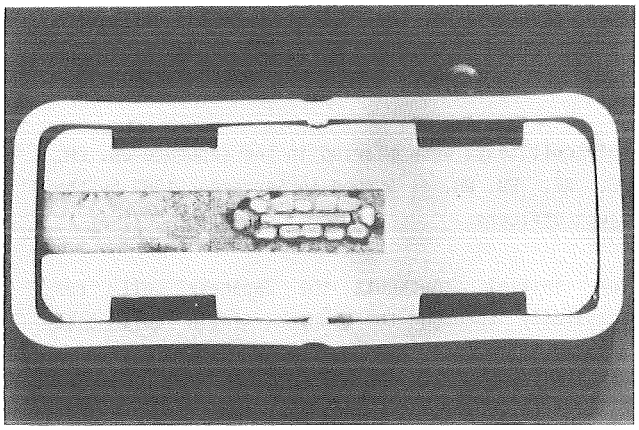

Fig. 20: The subsize Nb_3Sn conductor with NET-relevant design.

effectively ∿0.3%. The critical current to the flat cable is the same as for 7 single Nb_3Sn wires. b) The initial I_c for the flat cable + Cu is 15% lower than for the flat cable. This is due to the relatively large Cu cross-section (∿ 50%, i.e. somewhat larger than for a NET conductor) and to the soldering at 200°C, resulting in 0.1% additional prestress, c) the insertion into the steel case causes a further increase of prestress, leading to a further decrease of I_c, now 25% lower than for the flat cable. Such a degradation is larger than expected and reflects an excellent bonding between the Cu stabilizer and the steel case. The reasons of the important degradation of I_c after laser welding are not completely understood. Further tests on other configurations, even closer to the NET design will lead to a better understanding.

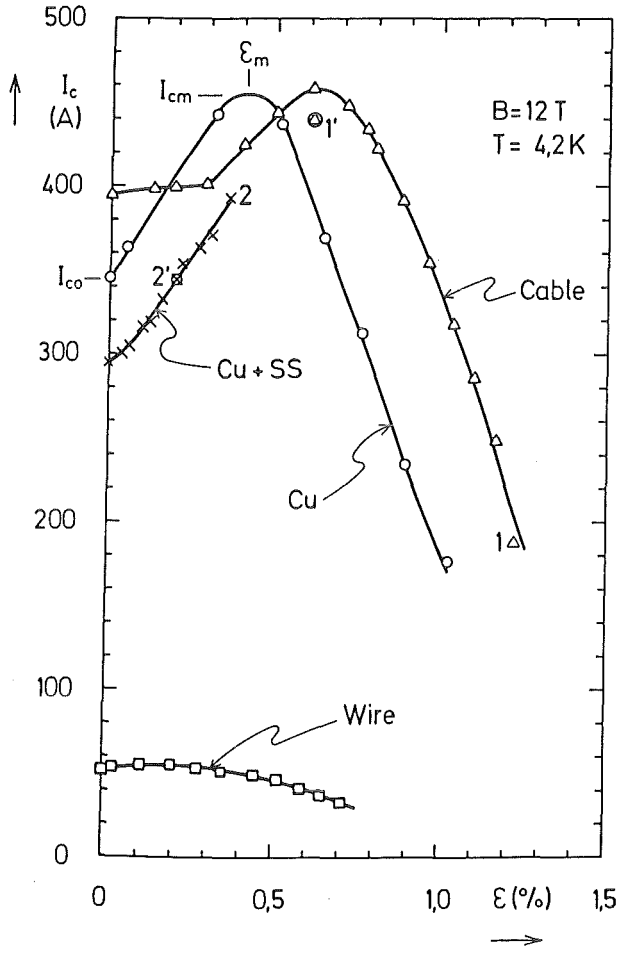

Fig. 21: Critical current vs. applied strain of all constituents of the subsize conductor

A new strain rig for measuring larger conductors up to 200 mm^2 cross-section at 12 T (100kN/6000 A) is actually being assembled and is expected to be operational during 1986.

2. Test in the HOMER High Field Test Facility

a) Tests in the 1.8 K Insert Cryostat

In the HOMER facility an 1.8 K insert cryostat was installed and used for conductor tests. The first investigations were focused to binary NbTi-conductors of a high manufacturing quality. These conductors have shown at 1.8 K, in the field regime between 10 to 12 T, higher critical current densities than those of Nb_3Sn, e.g. at 11 T a non copper j_c of 1.1 x 10^5 A/cm^2 compared to 6.5 x 10^4 A/cm^2 of a bronze route conductor was measured. These current densities and the easy mechanically handling of the ductile NbTi conductor are serious arguments for NbTi but with the handicap of a low temperature.

b) Mechanical Tests of Internal Cooled Conductors

Experiments with an internally cooled conductor of the type preferred in USA, the ICCS (bundle conductor), are in progress for comparison with the European designs. The first conductor under investigation is a small ICCS bundle conductor of 54 Nb_3Sn strands of 0.6 mm diameter embeded in a steel sheath of 6.7 x 6.7 mm^2 inner cross section and 0.6 mm thickness. First of all the aimed investigations should clarify the electrical stability behaviour of that conductor under simultaneous increase of current and forces or at least under constant current and increasing mechanical forces, similar to the situation in a real magnet. The helium content wetting the Nb_3Sn strands determines by its enthalpy mainly the stability and can be changed by a variation of the He pressure. Due to the fact that even the big bore of 260 mm diameter of the HOMER magnet permits only to generate stresses by Lorentz forces up to 100 MPa, additional forces have to be applied to get stresses of about 3 x 10^3 MPa and a strain up to 1% on the strengthened conductor as under real forces.

For this purpose the arrangement shown in Fig. 22 was designed and constructed. The idea is, to move outwards the segments of a subdivided disc by a conical piston pulled along the axis. The radial forces will be transmitted to the conductor loop at the circumference of the disc and will strain the conductor. Because these heat treated Nb_3Sn conductors cannot be bend over a diameter of 250 mm, the sample geometry must be fixed before the heat treatment which demands a well deliberated design including all steps of assembling.

Staff:

W. Barth
M. Beckenbach
M. Brünner
P. Duelli
U. Fath
R. Flükiger
S. Förster
F. Gauland
S. Gauss
W. Goldacker
A. Kling
B. Lott
G. Nöther
A. Nyilas
H. Orschulko
H. Raber
T. Schneider
W. Specking
S. Stumpf
P. Turowski

Publications:

V 21436
V 21619
V 21796

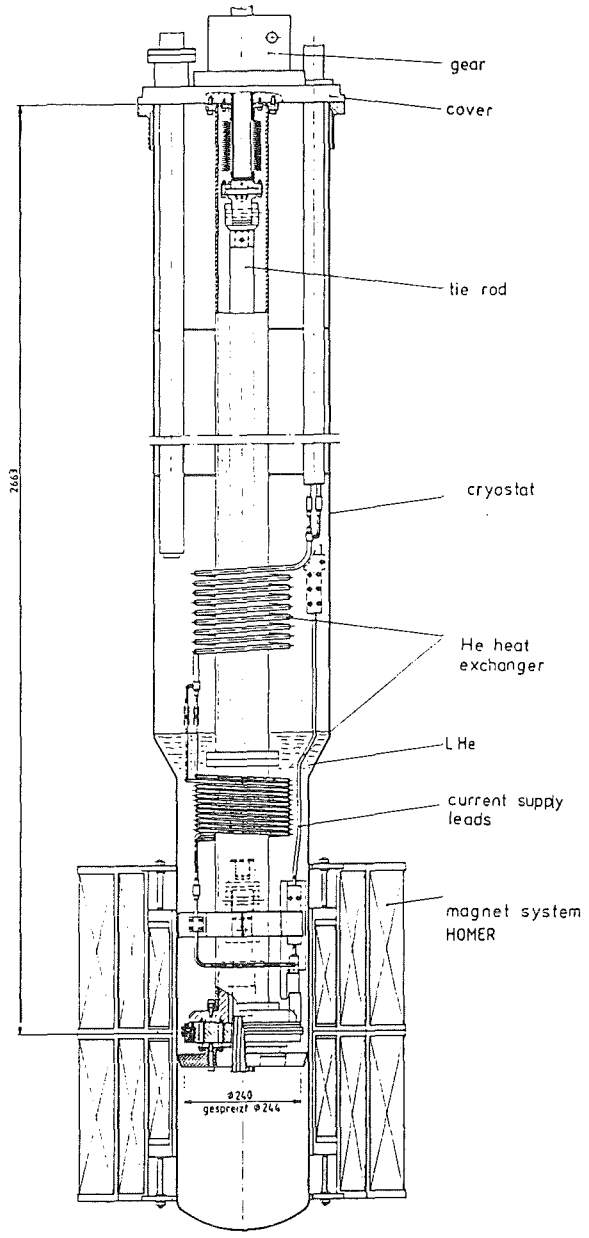

Fig. 22: The mechanical test arrangement in the HOMER magnet for investigation of internally cooled conductors

M 4 Superconducting Poloidal Field Coils

Superconducting Cable

Two contracts to develop the superconducting cable at industrial level have been placed to the European industry. The goal is to get 22 cable samples with length of 2 m to 6 m. Variations of the internal subcable insulation, the degree of compaction of the cable and the fabrication and welding procedure of the outer steel profile are foreseen. The samples will be investigated at KfK for mechanical and electrical properties.

Coil Design

The model coil design has been completed by the design of components like pancake connections current, feed throughs at the cable ends, and a design of the pancake connection area. A call for tender for the model coil is under preparation.

AC-Loss Measurements on Cable Samples

Measurements on cable samples have been carried out in order to determine the contact resistance between subcables if there is no subcable insulation at all. The contact resistance was measured for different degrees of compaction of the cable. The measured values reveal a fairly large contact resistance, so that even in this case the cable losses stay at a low level of typically 2.5 times the total subcable losses.

A superconducting dipole has been manufactured and installed in a cryostat to give high field change rates in order to investigate the stability behaviour of subcable loops. Currents will be induced in the ubcable loop by a pulsed superconducting solenoid. Measurements are under preparation.

2-Phase Flow Experiment in Existing TOSKA Facility

The experimental setup was finished and in January the first test started. Fig. 23 shows the flow schematic. We were able to measure adiabatic and nonadiabatic pressure drop with $\dot{m}$ = 2 to 8 g/s in the range of vapor content x = 0 to 1. The test section was also subjected to heat pulses in order to simulate the ac-losses during tokamak operation.

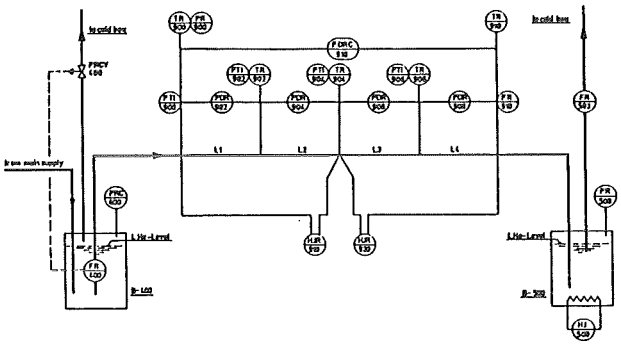

Fig. 23: Flow scheme of the two phase flow experiment

The pressure drop can be correlated by using the homogeneous model. Fig. 24 shows the results.

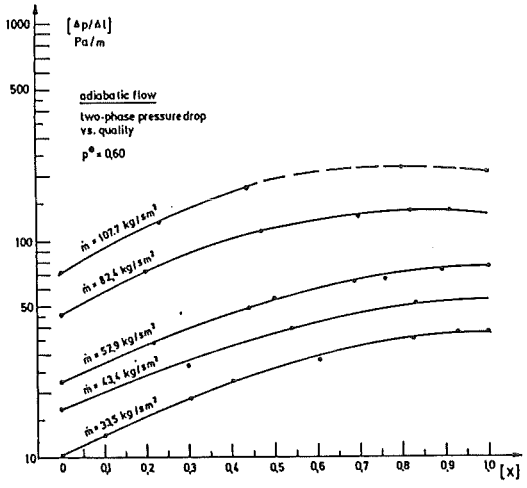

Fig. 24: Pressure drop as function of the He-gas content x

To gain more insight into the phenomena of two phase flow and the corresponding heat transfer, additional measurement devices will be installed. In particular, a special heated stainless steel pipe with thermometers around the circumference for detailed measurement of wall temperature, a viewing section to observe the flow pattern and a x-measuring cell which uses the different dielectric constants between liquid and gas are planned. The first two devices will be

provided by our collegues • from CEA who shall participate in the next experiments.
Future experiments will concentrate mainly on the effect of pulse heating and heat transfer.

Electric Power Circuit and Protection

A suitable electrical circuit for the tests has been rdered after final discussions with industry (Fig. 25). The modes of operation are charging and

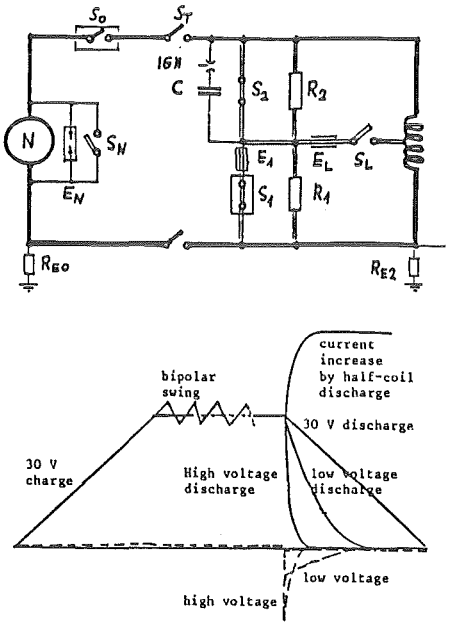

Fig. 25: Electrical power circuit as ordered at industry

discharging by a 30 kA/30 V power supply, low voltage and safety discharge at 900 V, high voltage discharge at 23 kV, half coil discharge to create 80 T/s field change in the other half, 23 kV discharge (1/3 Hz) to simulate the discharge cleaning in a tokamak, and 30 V/10 Hz bipolar swing of the power supply to generate ac-losses in the coil.

Quench detection and safety discharge have to be done in less than 0.6 s in order to limit the He pressure in the cable to 80 bar.

High Voltage Discharge

After charging the coil the current is transferred to a closed ac-vacuum switch S_2. This switch opens after the disconnection of the low voltage circuit (including the power supply) by the separator switch S_T and commutates the current into the resistor R_2 (S_1 closed). If S_2 fails, the safety switch S_1 is opened and the current is commutated into R_1.

Staff:

H. Bayer
F. Beckenbach
F. Becker
P. Duelli
S. Förster
G. Friesinger
U. Jeske
H. Katheder
P. Komarek
W. Lehmann
J. Lühning
G. Nöther
A. Nyilas
H. Raber
L. Schappals
G. Schenk
C. Schmidt
K. Schweickert
L. Siewerdt
E. Specht
H.-J. Spiegel
M. Süßer
A. Ulbricht
R. Wagner
D. Weigert
F. Wüchner

Publications:

V 21244
V 21435
V 21800
V 21957
21998
V 22407

M 9 Structural Materials Fatigue Characterization at 4 K

Joining Techniques for Structural Materials

For NET magnet structures and various supports at low temperatures materials have been preselected and joining techniques have been studied. These cryogenic materials have to preserve their low temperature performance with welds of up to 100 mm thickness. The welding procedure is a key controlling element for structural performance. The selected materials were three types of austenitic stainless steel. These were - in accordance with present LCT- and MFTF-experiments - 1.4429, 1.4435 and 1.4306 similar to 316 LN, 316 L and 304 L, respectively. It has been assumed that the welding technique for the magnet case manufacturing will be different from the past weld processes, such as the manual welding procedure. For the establishment of the welding technology a development programme has been worked out. This programme starts with 30 mm thickness and 1000 mm weld seam lengths of representative welds. To test materials weldability a clean weld process has been selected, i.e. TIG process with consumable wire. The wire will be premanufactured with the same heat of the procedured plate materials given above. To increase the deposition rate which is important for weld economics, the welding behaviour of preheated consumable wires will be tested. A call for tender for the development of the weld technology has been recently done. The institution "Schweißtechnische Lehr- und Versuchsanstalt, Duisburg" will develop the welding process according to the latest technological know how. The plate material manufacturing under the consideration of low phosphorus and low sulphur heats is under progress.

Cryogenic Test Facility

To proceed with the mechanical testings at cryogenic temperatures in an increased rate use of a small flow cryostat as a test device is intended. The design of such a mechanical test chamber has been completed. This flow cryostat will be adopted to the 20 kN mechanical tensile testing machine. The test chamber will allow the testing of compact tension specimens, tensile testing specimens as well as single edge notched specimens. The design allows to test multispecimens without warm up of the cryostat. In addition, the facility can test specimens under vacuum and at cryogenic temperatures. The effect of adsorbed gas on the materials fatigue crack growth at low temperatures will be measured. Fig. 26 shows the design of the flow cryostat. The load frame capacity of the cryostat is limited to 50 kN. A call for tender for the industrial manufacturing has been done.

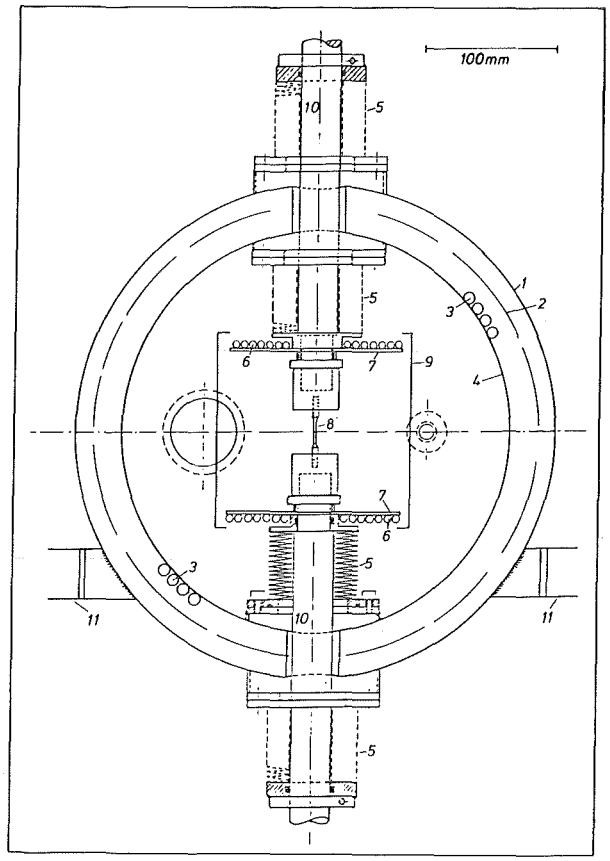

Fig. 26: Flow cryostat for mechanical testings
6) LHe-circuit, 3) LN_2-circuit, 8) specimen.

Staff:
G. Hohnburger
H.P. Raber
A. Nyilas

M 12 Development of Low Electrical Conductivity Structures

Joining of Fiber Reinforced Plate Materials

The use of fiber reinforced plastics as structural materials necessitates knowledge about the joint performance. To test the mechanical response of a joint, consisting of glass fiber reinforced plastic (GFRPP) and metallic materials, a design has been worked out. The load bearing element of the joints are metallic screws. The collapse load and the type of failure were determined for a simple GFRP/metallic screw bolted system at 4 and 15 K.

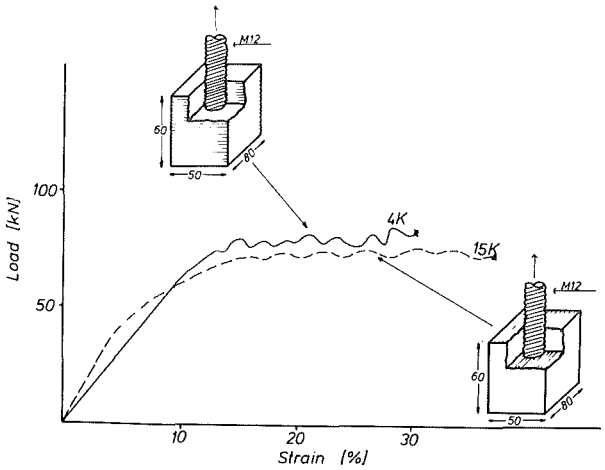

Fig. 27: Load vs. strain response of GFRP/metallic screw joint at cryogenic temperatures

Fig. 27 shows the yielding of the metallic material (Material 1.4301 similar to 304) and its typical serrated stress-strain behaviour. The failure analysis of the GFRP showed ply delaminations for the case of the thread machined perpendicular to the laminates. In case of the thread machined parallel to the laminates shear failure occured in the thread region of the GFRP. However, in both cases the bolts were fractured. According to the present design the operational load of the screw in direction of tension will be in the range of 25 - 30 kN. The safety aspects concerning the low temperature fatigue performance of such joints are important for engineering design. Further tests are under progress.

High Performance Fiber Materials

A development programme has been initiated to manufacture thick walled plate materials with S-glass. A call for tender is on the way. The industrial manufacturing of fiber reinforced plate materials incorporating metallic structures has been completed.

Staff:

G. Hartwig
G. Hohnburger
S. Knaak
H.P. Raber
A. Nyilas

MAT 1.9 Pre- and postirradiation Properties of 1.4914 Martensitic Steel

It is the main objective of the present task to investigate the influence of thermal cycling upon the lifetime of first wall materials. A thermal loading procedure is considered according to which the temperature oscillates between an "off-burn temperature" T=250°C and a "burn temperature" which is expected to be within 450°C and 650°C. The "burn time" is a test parameter which varies between 50 and 1000 sec; the "off burn time" is 50 sec. Two aspects of the problem have to be considered. With thermal cycling mechanical loading of the material is associated, which probably will cause fatigue. At the same time non-homogeneous temperature distributions may lead to crack formation which, despite of fatigue, will damage the material additionally. Therefore, the problem is investigated by two different methods.

1. The mechanical loading equivalent.
Assuming a homogeneous temperature distribution in the specimen, for particular boundary conditions, the mechanical loading, i.e. the stress/strain cycle, is determined from the corresponding thermal cycle. At constant temperature, these cycles will be applied to specimens, the lifetime of which is examined as a function of the strain amplitude and "burn time", respectively. Preliminary tests have been conducted on an austenitic ss which have shown, that the mean strain (i.e. whether it is tensile, compressive or zero) does not have an influence upon the number of cycles to failure. The tests will be started as soon as the specimens will be available.

2. Direct thermal loading.
A method was developed to heat a hollow hour-glass shaped specimen ohmically. Measurements have shown, that the pre-set loading conditions can be met. Additionally, radial temperature gradients can be generated and controlled by means of a gas flow through the tubular specimen. Moreover, the variable wall thickness of the specimen allows to investigate the influence of T-gradients on crack initiation and propagation for the same specimen. The electrical devices for automatical testing will be ready probably in September this year. In order to register the stress/strain diagram during thermal cycling, grips for the specimens are under construction which will also allow to conduct the experiments with free and fixed ends of the specimen, respectively. Preliminary tests with hand-driven loading are planned to study the formation of cracks on the surface of the test specimens in the course of thermal cycling. It is suggested to define the failure of the samples by appearance of cracks of a distinct size. An appropriate method for crack detection has to be developed.

Staff:
N. Baumgärtner
M. Bocek
C. Petersen
D. Rodrian
W. Scheibe
R. Schmitt
H. Schneider
W. Schweiger

MAT 2.2 In-Pile-Creep-Fatigue Testing of Type 316 and 1.4914 Steels

It is intended to study the in-reactor deformation and the fracture behaviour of the two candidate structural materials for NET with load cycling under tension.
The irradiation will take place in central position of the KNK II-reactor. Each irradiation rig will consist of eight pressurized tube samples which can individually be loaded by internal gas pressure and which is temperature controlled. Fig. 28 gives a view of a pressurized tube for such a cycling test.

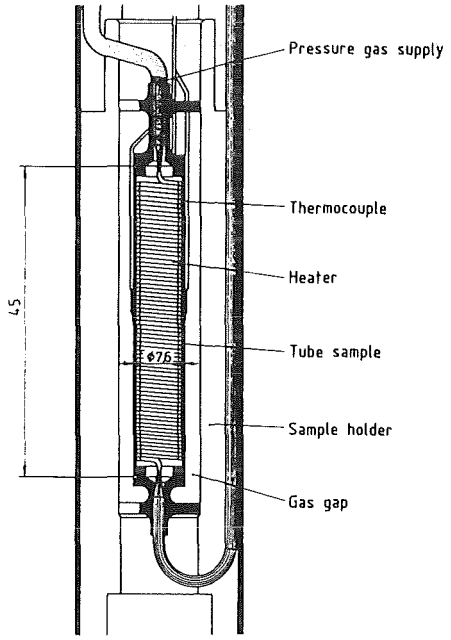

Fig. 28: Temperature controlled pressurized tube sample for load cycling tests in KNK II

The external parameters for these tests have now been specified. Sample temperature will be constant between 400 and 550°C, dependent on the reactor position. The inner pressure is variable between 100 and 450 bar, which corresponds for the given geometry of tubes to a maximum tangential stress of 400 MPa.
For the pressure control a first concept was developed and first experiments were started to measure the characteristic times for pressure increase and decrease. In Fig. 29 a typical pressure curve is given, indicating a pressure increase of about 10 to 20 bar/s. A pressure decrease of about 40 bar/s can be achieved. This figure is very suitable for simulation of stress-cycling in a Tokamak-type first wall.

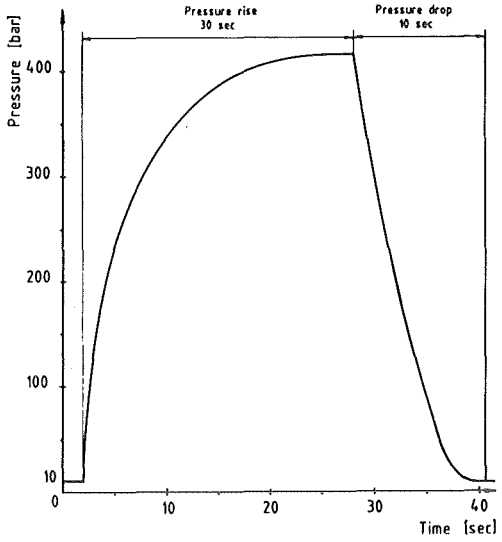

Fig. 29: Characteristic time changes of pressure for pressurized tube samples

Staff:
K. Ehrlich
L. Schmidt

MAT 6/MAT 13 Ceramics for First Wall Protection, Insulators and Windows

Common KfK-CEA irradiation tests in HFR-Petten (see the preceding semiannual report), OSIRIS-Saclay and PHENIX-Marcoule have been prepared or planned. Fast neutron doses will amount to 1 - 3 $x10^{22} n/cm^2$, irradiation temperatures will mostly be in the range of 400 - 600°C, but at about 1200°C for MAT 6 (first wall protection) ceramics in the HFR irradiation.

About 500 KfK specimens were made available, partly pretested, and assigned to the assembling maps. The specimen materials are HIP-SiC, CVD-SiC, three different qualities of Al_2O_3, and HIP-AlN. Special effort was devoted to measure the bending strength (with its Weibull distribution) of all these materials. Fig. 30 shows a Weibull plot of HIP-AlN. The mean strength values of the materials tested are given in Table 6.

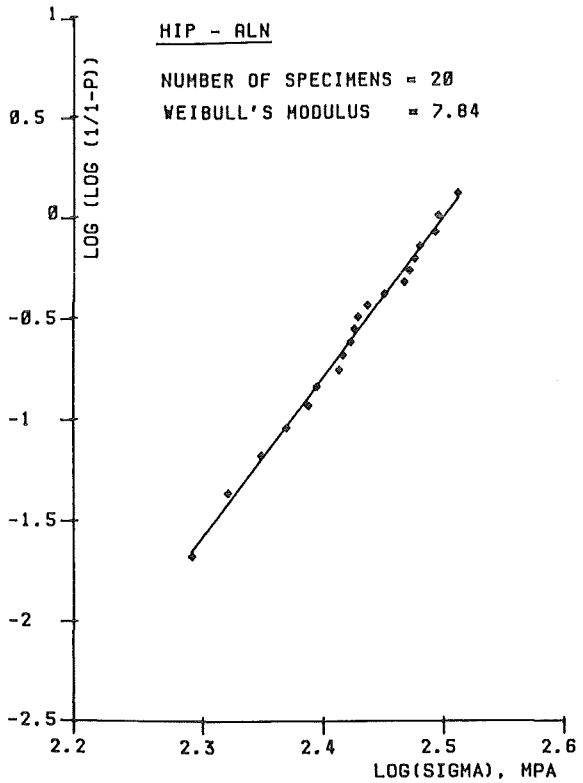

Fig. 30: Weibull plot of the bend strength of HIP-AlN

In order to characterize the electrical properties of the insulator materials, testing equipment was installed for measuring high D.C. resistance and complex dielectric constants in the MHz range. In

HIP-SiC	441 MPa
CVD-SiC	472 MPa
HIP-AlN	270 MPa
Al_2O_3 99,5%	204 MPa
Al_2O_3 99,9%	299 MPa
Al_2O_3 single crystal	355 MPa

Table 6: Mean bend strengths of the ceramic materials tested

contractual cooperation with the University of Karlsruhe, measurements of dielectric properties at about 35 GHz were initiated to classify the insulator materials for absorption in windows for ECRH of plasma.

The two types of polycrystalline alumina were used to perform measurements of the thermal conductivity λ. For both materials λ follows an equation of the type:

$$\lambda = \frac{1}{a + bT} .$$

"a" represents the minor influence of impurities, and the factor "b" differs by mo more than 5%. Up to 1000 K, is given by the correlation

$$\lambda = \frac{1}{- 0.00209 + 0.010428\ T/K} \quad W/cmK,\ 300 < T < 1000\ K$$

Staff:
Ch. Adelhelm
M. Blumhofer
W. Dienst
G. Gausmann
Ch. Gosgnach
H. Haase
R. Heidinger
B. Schulz
H. Zimmermann

MAT 9.2 Investigation of Fatigue under Dual-Beam Irradiation

1. Introduction

The Dual Beam Facility of KfK was developed as a research tool for materials within the European Technology Programme. The Dual Beam Technique allows the production both of damage and helium in thick metal and ceramic specimens by simultaneous irradiation with alpha-particles and protons of up to 104 MeV and up to 40 MeV, respectively. The facility described below is now under operation and has the capability of producing high amounts of damage (several dpa) and helium (several 1000 ppm) in bulk samples over a wide range of helium/damage ratios (1-10000 appm He/dpa).

2. Design and Construction Phase

The design phase had started in 1983 and included a) the design of the experimental hall (13x26 m) with the irradiation cell (4x8 m), b) the design of the two beam lines from the two existing cyclotrons to the cross point at the specimen, c) the design of the dual beam target station with the irradiation modules, and d) the design of the equipment (chambers, modules, control and computer electronics). In 1984 the construction phase had started and could be completed with respect to a) to c). In 1985 the installation of the equipment for performing the first irradiation shot in August 1985 had been done.

3. Testing Phase

3.1 Beam Testing

During the reporting period the installation of the dual-beam target station (see Fig. 31), of the monitoring instruments at the target station as well as of devices for remote handling in the separate control room had proceeded so far that the testing of the alpha-particle beam could be finished. This beam line is more difficult concerning the beam guidance. The testing of the proton beam is now under progress. In order to ensure a well defined beam quality special efforts were made: A beam diagnostic chamber contains diaphragms, beam profile grids and cooled Faraday cups with secondary electron suppression. Additionally a beam energy moderator was mounted into the alpha-particle beam to degrade the energy from 104 MeV to zero continuously in order to achieve a homogeneous helium implantation profile. For simultaneous measurement and absolute analysis of both beam profiles a new diagnostic system was developed and tested successfully. In addition a sandwich-moderator was developed considering the lateral straggling at low energies with the aim to reduce the irradiation time significantly.
The guidance of the initial beam is undertaken optically by a camera supervising system for a set of mirrors.

3.2 Target Testing

A complex heating system was built to guarantee a homogeneous temperature profile at the specimens under different irradiation conditions. For removing the irradiation-induced heat deposition in tubular specimens developed for LCF studies, a helium cooling loop operating at 2 bar with gas velocities near sound velocity was built. The construction of a high vacuum and high temperature oven for an INSTRON testing machine was completed. At present all these devices are tested and will probably go into operation during the next reporting period.

3.3 Process Data Acquisition

The experiment can completely be operated in a manual as well as in a remote mode. All signals coming from or going to the experiment are monitored by a process computer. The wiring of the handware has been completed and the programming of the software has been started. The computer-controlled operation of some units could successfully be demonstrated. The processing of the data acquired by the process-computer is foreseen by means of a central computer linked to the front-end processor via a local area network.

4. The Experimental Phase

In order to test the experimental equipment under real conditions a small experimental programme has been set up. A set of sheet specimens made of type 1.4914 martensitic steel was homogeneously implanted with alpha-particles in the temperature range 600-750°C. Their tensile and creep properties will be tested during the next reporting period and compared with reactor irradiations. The next experimental step is the testing of an irradiation module for LCF-specimens and the start of the irradiation of tubular specimens is planned.

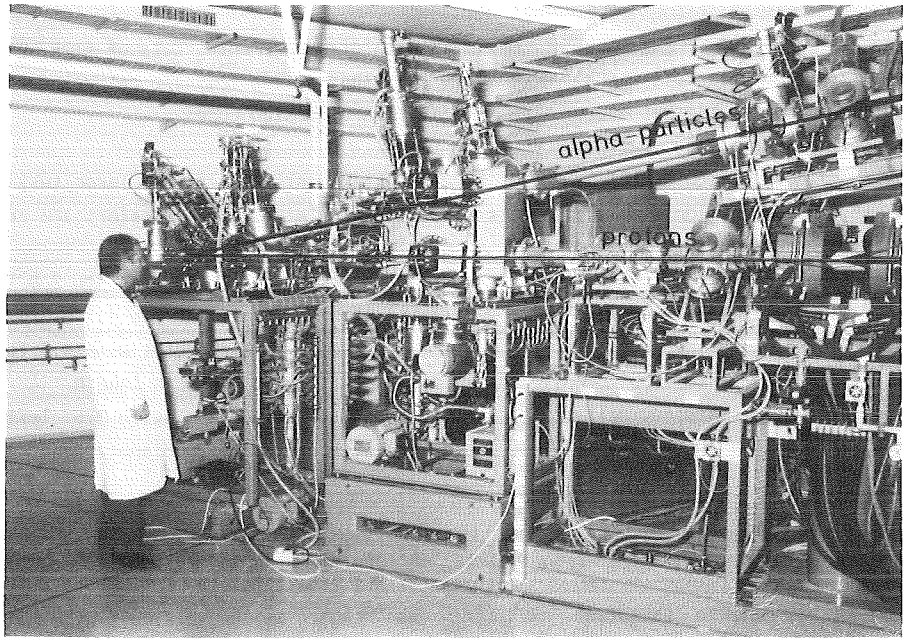

Fig. 31: Side view of the two beam lines with the diagnostic- and experimental chamber

Staff:	Publications:
G. Bürkle	20214
S. Heger	21384
D. Kaletta	21395
A. Möslang	21495
D. Preininger	22398
G. Przykutta	V 22399
A. Will	

N 5 Development of Theory and Tools for Evaluation of Magnetic Fields Effects on Liquid Breeder Blanket

Magnetohydrodynamic effects are of paramount importance for Liquid Metal Fusion Blankets (LMFB) especially, if selfcooled liquid metal blankets are considered. This is because the interaction between the high magnetic fields and flowing liquid metals results in large body forces exerted on liquid metal. To overcome this MHD body forces large pumping pressures must be applied on the liquid metal coolant. This does not only require large parasitic pumping power but may render the containment of the coolant impossible. If for example the MHD pressure drop can not be minimized by appropriate design features, self-cooled liquid metal blankets will become impossible.

Therefore, an MHD-program was started at KfK. In order to support the experimental investigations theoretically and to gain deeper insight into the MHD phenomena, a literature survey was made to establish the state of the art in MHD. First attempts to simulate MHD-flow in simple geometries yielded satisfying results but also revealed the limits of the used simple procedures especially with respect to the spatial resolution needed.

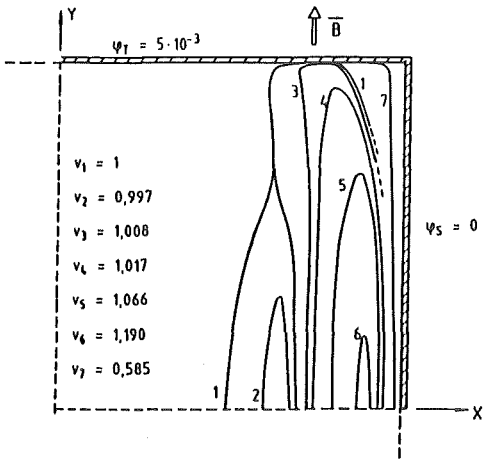

Fig. 32: Numerically calculated isolines of velocity

As an example, Fig. 32 shows the numerically calculated isolines of velocity in the first quadrant of a rectangular duct for a Hartmann number of 10^3. The corresponding experimental part of the MHD-program is aimed to deal with the following topics:

- verification and/or improvement of existing scaling laws,
- acquisition of experimental data of flow geometries where existing scaling laws are not valid,
- verification of design codes.

To conduct experiments with rather large test volumes, three magnets with different parameters are procured:

- a normal conducting dipole magnet with 2.0 Tesla and a test volume of 0.17 m x 0.5 m x 1.3 m
- a superconducting dipole magnet with 4.5 Tesla and 0.06 m in diameter and 1.0 m in length
- a superconducting solenoid with 3.5 Tesla axial field strength and 0.4 m in diameter and 1.0 m in length.

With respect to the scaling of the experimental results of NET conditions the sodium-potassium alloy $Na_{22}K_{78}$ was chosen as the working fluid. It can be operated at room temperature. The design of the NaK test loops is accomplished. The main components like pumps, tanks, valves, flowmeters etc. are ordered.

The first experimental setup which will be used to measure the MHD pressure drop in a straight duct is shown schematically in Fig. 33.

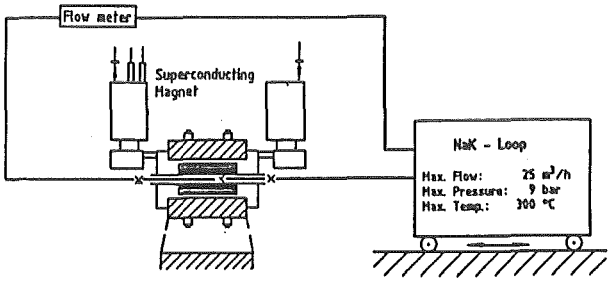

Fig. 33: Schematic outline of the experimental setup to measure the pressure drop in straight ducts

Interpretation of MHD flow requires knowledge of flow pattern. Well known measuring methods such as Pitot-tubes and hotfilm anemometer can not be applied when a strong magnetic field is in action or they only have a low sensitivity. The calculation of flow velocity from measured voltage in the flow is not possible under all conditions. Therefore, in KfK, a velocity meter is in

development using the "temperature pulse propagation time" method (TPPT). It uses the measurement of propagation time of temperature waves and their height to evaluate the magnitude of local velocity and its direction. The probe consists of a miniaturized heater with an outer diameter of 0.5 mm. It is pulsed with an energy rate of 60 Wsec/m and a pulse time of 1 msec. In a distance of a few mm thermocouples are positioned to detect the propagation time of the temperature wave and its height. The thermocouples with an outer diameter of 0.25 mm have BN as insulating material in the area of the hot junction. Their response time is $\leq$ 2.5 msec.

The temperature waves propagate by conduction and convection. For liquid metal at low velocities with their high diffusivity of heat (a) the contribution of conductivity on propagation time is not negligible. Therefore, both components have to be regarded to convection velocity v of the liquid metal can be calculated from the measured propagation time (t) of the temperature wave maximum by

$$v = \sqrt{\frac{r^2}{t^2} - \frac{4a}{t}}$$

when the temperature wave is generated along a straight line in a very short time (thermal explosion). Fig. 34 shows a photo of a sensor head with one heater in the centre and 8 thermocouples placed in a distance of 2 and 4 mm around the heater, respectively.

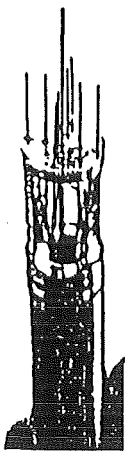

Fig. 34: Sensor head

To detect the very weak signals, an amplifier has been developed with an amplification of 1.3×10^5, high response time and low noise (0.01 K when the thermocouple is connected). A typical measuring curve is shown in Fig. 35, taken in stagnant mercury. Testing of all components of the measuring system (heater, sensors, power supply, amplifier) was carried out both in solid copper and stagnant mercury.

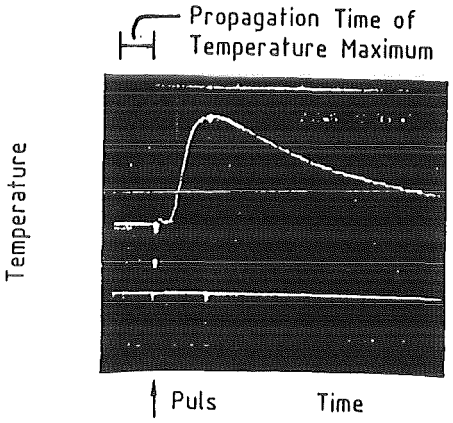

Fig. 35: Temperature pulse

System			Copper		Mercury	
temp. propag. path		[mm]	4-5	5-6	4-6	2-4	2-4
propag. time	measured	[msec]	22	24	46	576	576
	calculated	[msec]	19	21	42	536	536

As the comparison of measured and calculated propagation time shows, a good agreement can be stated.

Staff:
G. Arnold
L. Barleon
V. Casal
H. Kreuzinger
H. Kußmaul
K.-J. Mack
A. Sterl

RM 3 Handling Equipment for In-vessel Components

Inspection, repair, and replacement of NET in-vessel components require special remote handling equipment. The organizations CEA, CEN/SCK, ENEA, and KfK cooperate in the development of such equipment. The development is oriented towards handling of the following components: protection tiles for the first wall, divertor plates, active coils, and radio-frequency antennae. These components are considered as typical for all other remote handling work that will have to be carried out inside the vacuum vessel. The principal equipment for the task is called "In-Vessel Handling Unit". It consists basically of:

- a contained transfer unit,
- a transporter (which will likely be an articulated boom or some other carrier system serving the same purpose),
- front end effectors to be attached to the carrier such as a manipulator device and special handling units.

The whole development programme for the In-Vessel Handling Equipment consists of 9 subtasks:

1. Evaluation of a conceptual design for in-vessel remote equipment.

2. Conceptual design and demonstration of an overall geometry inspection system.

3. Conceptual design and demonstration of an optical tracking device for component insertion and withdrawal.

4. Conceptual design of a device for the exchange of tiles.

5. Conceptual design and demonstration of a system for divertor plate alignment.

6. Definition of a system for boom position monitoring.

7. Definition of a welding system for repairing the bellow covers of the vacuum vessel.

8. Radiation hardening of basic components.

9. Feasibility analysis of the handling unit as a function of operating temperature (100° and 150°C).

KfK participates actively in the subtasks 1, 2, 4, 6, 7, 8 and 9. The work is being performed in close cooperation between the KfK Institutes IDT, IRE, and IT.

At this time, the following status of work has been achieved:

Sub-task 1: Development of Concepts

Based on the analysis of the JET articulated boom, the preliminary results of the development project for the TFTR articulated boom, initial studies of various kinematic link chains were undertaken. Five principally different options were selected for more detailed analysis. They are distinguished from each other basically with respect to the vessel access method (horizontal versus oblique vertical access, e.g.). Besides kinematic design criteria, aspects of joint loads and safety will be considered next.

Sub-task 2: Overall Geometry Measurement

Various technical solutions for remote geometry measurement were investigated and compared. The main aspects of the comparison were the accuracy requirements, the overall dimensions, speed of measurement, integration of the measurement into a CAD data base, and the technological development potential. A triangulation method based on lasers was selected. Equipment for a demonstration test was ordered. The interface between the measuring system and the CAD data base was defined.

Sub-task 4: Tile Exchange

Preliminary investigations of this task were initiated. This task will benefit significantly from the activities oriented towards the modification of the TFTR protection tiles for remote handling.

Sub-tasks 5 through 9

During the first phase of the investigations, these sub-tasks will be treated in common. All these tasks require an investigation of the potential sensor technique. The selection of sensors to be used for NET requirements will be delayed until the common study

has been performed. CEN/SCK and KfK have agreed to approaching these tasks in a coordinated fashion with a goal of preparing a common report on the state of the art.

Sub-task 6: Boom Position Monitoring

In support of the activities for NET, KfK participates in the development of the remote handling control system for JET. In particular, KfK develops a computer graphics supported man-machine interface for the remote control of the JET articulated boom (a "graphical master"). The graphics workstation will give the remote handling operator an overview of the present handling situation, including the status information from boom position sensors. The concept includes processing of geometry data for collision avoidance. The system is to undergo its first field test during the shutdown period of JET in winter 1986/87. The installation at JET will serve as a demonstration site for the boom monitoring system to be developed for NET.

Staff:
H. Becker
J. Benner
G. Böhme
H. Breitwieser
E. Holler
J. Hübener
J. Isele
H. Knüppel
W. Köhler
I. Kornelson
U. Kühnapfel
K. Leinemann
H.A. Rohrbacher
E.G. Schlechtendahl
J. Schröder
M. Selig
A. Suppan
W. Weber

S+E 1 Radioactive Effluents in the System Plant/Soil

The installation of the climatic chamber for exposure of plants to gaseous tritium has been finished. First functional tests were carried out successfully.

A working scheme for separation of organic plant material to its main components has been developed. The methods (1, 2, 3, 4) were tested with inactive plant material. Free tissue water can be received by freeze drying. Organically bound tritium (OBT) will be determined by oxidation of dryed plant material in an automatic oxidizer and measurement of HTO by liquid scintillation counting. The oxidizer will be delivered in the next future.

Preparations for the French Tritium Release Experiment taking place in May or June 1986 are going on. The KfK experiments include the exposure of plants and soil cores from Germany to the released HT and the installation of two devices for measurement of HT and HTO in air at the position of the soil and plant samples during the exposure.

A sampling system for collecting HT and HTO in the environmental air (Fig. 36) has been completed and verified with tritium gas. The first molecular sieve traps retain atmospheric water and HTO. Then the air stream goes through a Pt catalyst to oxidize HT to HTO which is retained in two following molecular sieve traps. In order to provide sufficient sample in the traps after the catalyst, excess of H_2 is added to the air stream (0,1 % by volume). The flow rate is 50 l/min. For measurement of the retained HTO the molecular sieve is charged with unlabeled H_2O that exchanges with HTO. The activity is determined by liquid scintillation counting.

Future activities:

- Accomplishing of a measuring program of tritium background on the site of the planned tritium release experiment.
- Participation in the release experiment, analysis and interpretation of the received soil, plant and air samples.
- Preparation of the climatic chamber for active tests with HT, installation of measuring equipment to analyze the chamber air for HT and CO_2. Inactive tests with H_2.
- Production of plant material universally labeled with tritium in order to test the separation methods for organic material.

References:

1. Basha, S.M.M., Plant Physiol. 63, 301-306 (1979)
2. Hari, V., Anal. Biochem. 113, 332-335 (1981)
3. Marmur, J., J. Mol. Biol. 3, 208-218 (1961)
4. Stein, D.B. and Thompson, W.F., Plant Science Letters 11, 323-328 (1978)

Staff:
S. Diabaté
D. Honig
L. König
H. Schüttelkopf

plant material

cut to pieces and lyophilized

- homogenization in 10 mM Na_2EDTA, 500 mM NaCl, 10mM Tris pH 8,4, 1 % SDS at 60°C and holding at 60°C for 30 min
- cooling to 37°C and adding of pronase, 10 mg per ml homogenat, incubation at 37°C for 2 h
- centrifugation
- the supernatant fractions are adjusted to 1 M with respect to $NaClO_4$ and shaken with an equal volume of chloroform/isoamyl alcohol (24:1, v/v)
- recovering of the aqueous phase after centrifugation
- repeating of chloroform/isoamyl alcohol extraction for several times
- precipitation of nucleic acids with 2 volumes of ethanol at - 20°C overnight
- centrifugation

nucleic acids

- dissolving in a small volume of 20 mM sodium acetat, 100 mM NaCl, 10 mM Tris pH 7,5
- cesium chloride density gradient centrifugation

DNA | RNA

- further separation by electrophoresis

- homogenization in 70 % acetone containing 0,1 % mercapto-ethanol at - 20°C
- centrifugation
- repeating of this procedure for several times
- drying

- extraction of proteins with 9,5 M urea, 5 mM K_2CO_3, 2 % Nonidet P-40, 0,5 % mercapto-ethanol
- centrifugation

proteins

- further separation by SDS-acrylamid-gel electrophoresis

- evaporation of acetone extracts
- extraction with n-hexane

fats and pigments

- adding of 2 volumes of ice-cold acetone containing 0,1 % mercaptoethanol to the super-natant fractions, 1 h at -20°C
- centrifugation
- washing of the final pellet twice in 70 % acetone, 0,1 % mercaptoethanol
- resuspension in 10 mM Tris, pH 7,4, 5 mM $MgCl_2$, adding of DNase and RNase at 50 µg/ml each, incubation for 30 min at room temperature
- acetone precipitation

cell walls

- washing with water for several times, finally with acetone
- drying

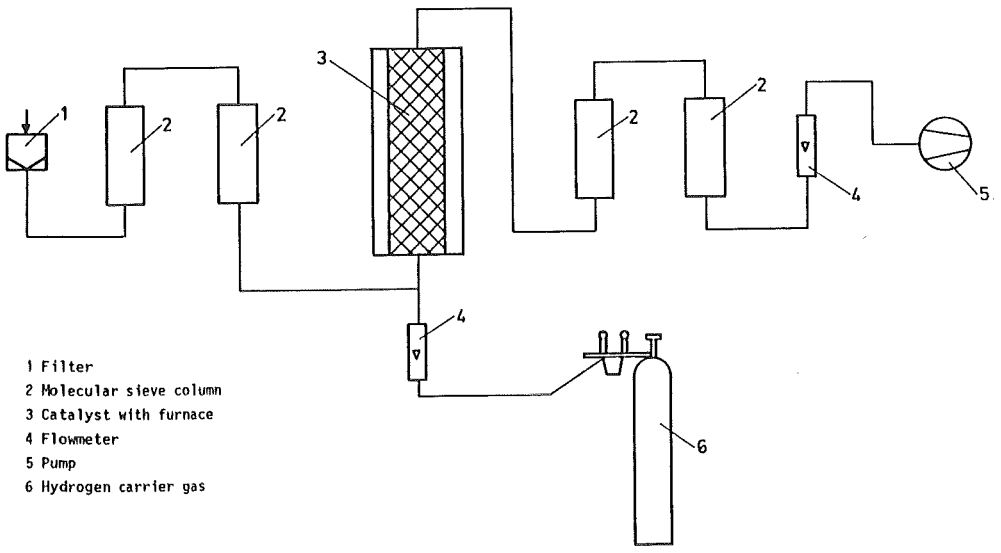

Fig. 36: Schematic representation of HT/HTO sampling system (preliminary)

S+E 4.1.2 (S+E 2) Safety Aspects of Cryosystems

Buckling Behaviour of the Cryostat

In order to investigate the buckling behaviour of the cryostat a simplified strategy for the analysis of linear elastic stability problems was proposed.

So far the simplified approach has been tested by application to simple stability problems and comparison with alternative solutions. To clarify the quality of this simplified approach a general theoretical assessment has been performed for thin shells with arbitrary geometry either under hydrostatic pressure or dead loading along the boundary. It was possible to derive general approximate solutions for the actual stability problem (eigen value problem) as well as for the simplified approach (linarized boundary value problem of imperfect shells), which allows a direct comparison. Although similarity in the expressions for the critical load factors is obtained, it turns out that the simplified strategy cannot generally be expected to predict the actual critical load factor. This result is in contrast to the observations made for some simple stability problems where agreement has been found.

Therefore, during the past period to be reported here, additional, more complex sample cases of linear stability problems have been investigated. Especially it has been examined, whether the sometimes strong influence of different boundary conditions on the buckling load can be accounted for by the simplified approach. For a lateral compressed cylindrical shell eight different boundary conditions have been considered. Compared to numerical results from the literature the tendency of the influence of different boundary conditions is correctly predicted. However, deviations up to 20 % in the load factor are found. The causes of these deviations are not yet understood, but following the general result of the mathematical analysis, their presence is to be expected. These investigations have to be continued. A future goal will be to find those classes of linear stability problems where the proposed simplified approach yields acceptable results.

Staff:

B. Dolensky
R. Krieg
T. Malmberg
S. Raff

S+E 4.1.3 (M 1) Safety Aspects of Superconducting Magnets

Staff:
P. Duelli
W. Geiger
A. Grünhagen
L. Hütten
K.P. Jüngst
H. Kiesel
G.W. Leppelmeier
G. Obermaier
H. Schnauder
F. Spath
M. Steeves
E. Süss
A. Wickenhäuser

Publication:
V 21327

In the first step the TESPE-S magnet safety programme mainly consists of the investigation of different fault operations with each fault being studied separately. This procedure has to precede later destructive experiments in order to accomodate them safely and to interpret their results.

Experimental results of buckling measurements, taken at last period, measuring of the TESPE torus were further evaluated. They demonstrated the potential for buckling measurements as a suitable tool for the detection of mechanical changes in the system during current operation.

A first "loss of vacuum" experiment up to 500 Pa was performed. Experiments with higher pressures require reconstruction of the helium venting line to enlarge its capacity.

The torus experiment with one coil short-circuited across its terminals was run successfully. Good agreement was found between experimental data and calculations. Both current ramping up and down led to critical phases of operation. Running the current down induces an over-current in the shorted coil, while increasing current induces a counterflowing current in the shorted coil, which thereby experiences a force in radially outward (!) direction.

The asymmetric 5-coil experiment was run with currents up to 5000 A. In addition to currents and voltages movements of coils and asymmetric forces were measured.

A theoretical study on safety of magnet system components was started in continuation of reliability analyses for subsystems in fusion facilities. First object is the control system of the energy dump circuit of superconducting magnet systems. For the top event "no current interruption on demand" the TESPE-S facility has been analysed as a first example. Because of lack of reliable probability data for some prototype components, the strategy is to identify the critical cuts. This method was successfully applied earlier to the analysis of the protection system for a neutral beam injector. Next step of analysis includes the dump circuit of NET.

T 6 Industrial Development of Large Components for Plasma Exhaust Pumping

Staff:
J. Hanauer
W. Höhn
U. Kirchhof
H. Lukitsch
A. Mack
D. Perinić

1. Component Development

The Fusion Technology Steering Committee (FTSC) approved the contract on the feasibility study for the turbomolecular pumps (TMP). The contracted company will start the investigations in April 86. The final results of the study will be available twelve months later.

The bidding procedure for the feasibility study on the all-metal gate valves, ND 1500 mm, is terminated. Four companies have sent quotations. A contract proposal is being prepared and will be submitted to the FTSC for approval.

The technical specifications elaborated for T6 are based on the NET operational data defined in 1984. In the meantime, important NET requirements have been reduced (power, burn time ...). Before launching the prototype construction in 1987 it will be necessary to redefine the basic target of T6. It has to be decided if the components to be developed in task T6 shall address DEMO specifications or the somewhat relaxed NET specifications should be considered as the target.

A time schedule was elaborated for prototype development, industrial construction of components and assembly of the plasma exhaust pumping system. The prerequisite of construction to schedule (i.e. in 1998) of the pumping system is start of prototyping in the years 1987 to 1989.

2. Component Testing

The feasibility study for the large component test facility is completed. On account of the potential necessity to use tritium in prototype testing, the site selected for the testing facility is adjacent to the tritium laboratory of KfK.

The costs have been estimated for different alternative testing facility concepts. They vary between DM 2.7 million and DM 4.6 million for the building and between DM 4.5 million and DM 6.9 million for various testing facility concepts. For tritium operation additional investment costs between DM 3.4 million and DM 5.3 million have been calculated.

T 10 H Plasma Exhaust Purification: Catalyst Development

Present concept under consideration for the removal of impurities from the plasma exhaust of a fusion machine foresee the employment of a Pd/Ag alloy diffuser for the separation of the process gas into a pure heavy hydrogen fraction, fed into the isotope separation system, and a noble gas stream, containing up to 15% of tritiated and non-tritiated impurities.

At KfK a process scheme for the recovery of tritium from the impurity fraction is presently being examined experimentally. For this purpose a laboratory loop, shown schematically in Fig. 37, has been constructed. Main components of the loop are a Pd/Ag diffuser, a buffer vessel and a catalyst vessel. Gas analysis is carried out with a gas chromatograph and/or a quadrupole mass spectrometer.

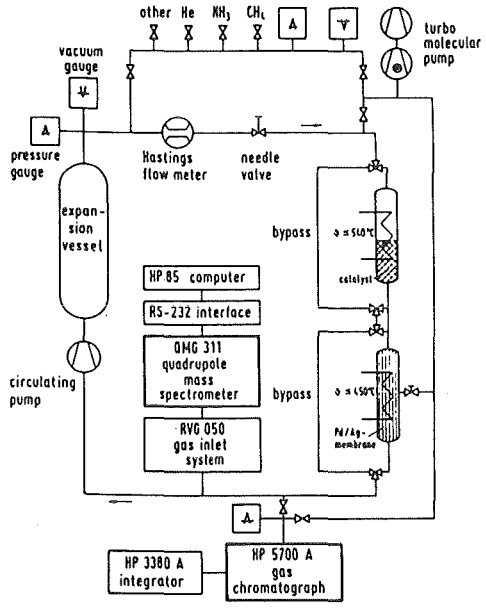

Fig. 37: Schematic view of the experimental arrangement for the investigation of catalytic reactions

Employing He as a carrier gas it was shown that on a suitable Ni catalyst, at temperatures in the range 350 - 450°C, NH_3 can be readily decomposed into the elements N_2 and H_2. The decomposition reaction obeys the rate equation

$$-\frac{dNH_3}{dt} \sim \left(\frac{P_{NH_3}{}^2}{P_{H_2}{}^3}\right) \quad 0.43$$

High flow rates (120 l/h) were selected in this study. Under these conditions the conversion per pass through the catalyst bed is low and the loop can be treated as an ordinary batch reactor. The results show that at 450°C in accordance with thermodynamic prediction the equilibrium

$$2\ NH_3 \rightarrow N_2 + 3\ H_2$$

is far at the right. If, in addition to catalytic decomposition, hydrogen is continuously extracted from the loop with the help of a Pd/Ag alloy diffuser, the rate of the reaction is accelerated and the conversion becomes quantitative.

The experiments show that the decomposition of NH_3 can also be carried out directly inside the Pd/Ag alloy diffuser at 400°C. The reaction is very effective. As shown for example in Fig. 38, when a gas mixture of He with about 10% by vol. of NH_3 in a 5.2 l vessel is circulated over 0.12 m^2 of a Pd/Ag membrane at a flow rate of 0.3 l/min, 90% of the hydrogen bound to NH_3 can be extracted from the loop by permeation in a period of 3 hours. The only reaction product remaining in the loops is N_2. Under more optimized conditions a much faster and efficient recovery of bound hydrogen (tritium) should be achievable.

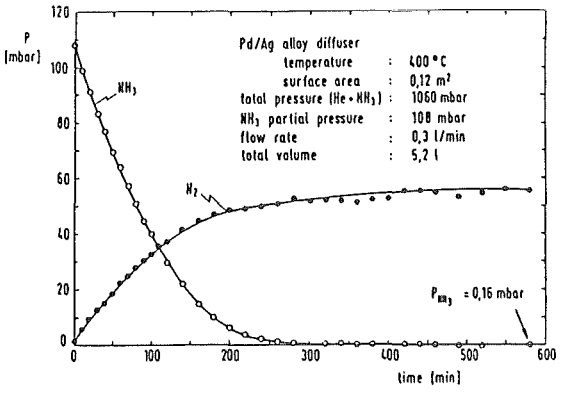

Fig. 38: Cracking of NH_3 in a Pd/Ag alloy diffuser

CH_4 can also be decomposed at 450°C into H_2 and graphite on a Ni catalyst. The reaction is reversible. If the catalyst bed is operated in conjunction with the Pd/Ag diffuser, 100% conversion is possible. This was demonstrated in experiments with up to 15% by vol. of CH_4 in He. Carbon depositing on the catalyst does not appear to have a marked inhibitory effect. With excess hydrogen at appropriate temperatures

superficial carbon will react to form CH_4. Therefore, extended use of the catalyst can be expected.

Staff:
M. Glugla
K. Nolte
R.D. Penzhorn
P. Schuster

T 12 Removal of Tritium from Breeding Blanket

A scoping study has been performed for the solid breeder as well as for the liquid breeder blanket alternatives of KfK. The study was started under task B1, the progress report is given under this reference.

Studies for NET/INTOR

A draft of the study "Vacuum Tight Connections and Closures on the Vacuum Vessel-Lip Welding and -Cutting" was presented to the NET-Team. Some extensions have been agreed in the discussions. They concern the establishment of a relatively detailed R & D programme and a more detailed investigation of the JET-Lip welding and -cutting system. The experience gained by JET in the meantime will be taken into account. The final report is under preparation, it will be available end of April 1986.

The study "Pipe and Vacuum Duct Connection" was completed and presented to the NET-Team. After some modifications especially in respect to the comparison of the different types and the proposal of the R & D programme, the final report was issued end of February 1986.

The output of the study is the basis of the Association Contract No. 205-85-1 FUAD/RM1 - "Background Studies/Pipe Connections" which has been launched in the meantime.

The study "Stress and Lifetime Calculations" has been continued. For the actual NET first wall with inner cooling channels temperatures and thermal stresses were calculated by use of the Finite-Element-Method. Due to the cyclic reactor operation these stresses become also cyclic. The longtime changes of stresses during operation causes by irradiation creep and swelling was considered. First lifetime calculations were performed assuming edge cracks situated at different locations of the structure:

Fig. 39 shows the cyclic stress intensity factor ΔK - the driving force of the propagating crack - at the plasma facing side and the backward part for a crack with an initial depth of 0.1 mm.
It can be concluded, that the backward part is the weakest point of the structure. If martensitic instead of austenitic steels are used, the lifetime of 1st wall components can be increased.

The NET TF Coil Design Study was continued with the aim of identification of critical paths and components for design and construction of the toroidal field coils and by preparing solutions for the identified problems.

In the period under review finite element calculations

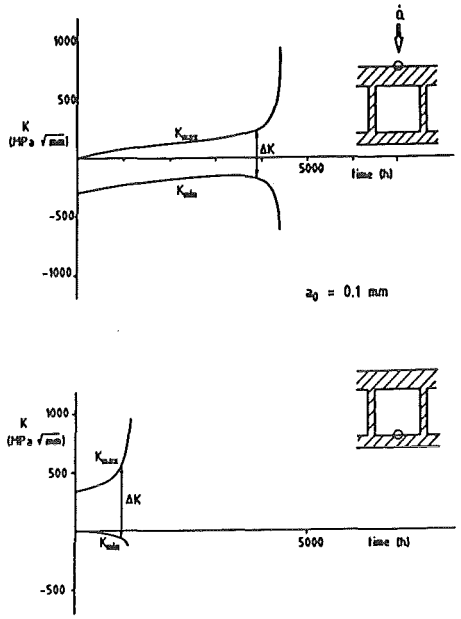

Fig. 39: Stress intensity factors for two cracks situated in the front part and in the backward part of the wall

on torus components and modifications and model design of the superconductor have been elaborated.

The superconductor cross section was adapted to new NET parameters. Arguments of manufacture led to alteration of the stabilizer, which now will be prefabricated and soldered to either side of the flat superconductor. The concept of high stability and low a.c. losses was kept.

A subsize conductor was defined the fabrication and test of which is to verify the conductor design (see M3).

For the torus a vault structure is required with a significant part of the arising toroidal forces being carried by the winding pack. Implications on conductor and coil design have been investigated by finite element analysis. Optimization calculations for coil and casing geometries were started taking into account the load on superconductor and casing, the shear within the winding pack and between windings and casing, and the required free space at the inner and outer radii of the torus.

Concerning the Scoping Study on Structural And Insulation Low Electric Conductivity Materials for NET-Magnetic Systems the part "Radiation Damage to

Polymers and Fibre Composites" has been finished. The degradation mainly of mechanical parameters, but also of electrical and thermal properties by irradiation was reviewed. The results of many papers have demonstrated that several types of polymeric materials are sufficiently resistant to a radiation dose typical for fusion reactors. They are therefore applicable in fusion technology with respect to their stability against irradiation. In the first quarter of 1986 the review on electrical, thermal and gas permeation properties of those materials have been complied. Measurements of material properties were performed on a test-element designed for a coil-casing made out of carbon fibre composite materials.

Staff:
G. Böhme
E. Diegele
K. Ehrlich
T. Fett
R. Flükiger
B. Haferkamp
G. Hartwig
K.P. Jüngst
P. Komarek
M. Kuntze
K. Leinemann
J. Lühning
A. Ludwig
R.A. Müller
D. Munz
A. Nyilas
M. Selig
F. Spath
K. Stamm
E. Süss
E. Ternig
A. Ulbricht

Development of ECRH Power Sources at 150 GHz

The aim of this task is to demonstrate the feasibility of a high power gyrotron type microwave generator at a frequency of 150 GHz. Studies to be carried ot on a modular test gyrotron address in particular the possible coexistence of modes (mode competition), excited by the electron beam in the oversized resonator.

1. Gyrotron Test Facility

The preparation of the test facility for the initial gyrotron experiments was terminated. The short pulse ($\sim$10 µs) high voltage supply and the new hv interface for measurement and auxiliaries are in operation. The cryogenic supply system for the superconducting magnet has been completed by adding the compressor. The instrumentation in the control room has been extended.

The series modulator fabricated commercially was pre-tested in the factory and delivered to the KfK gyrotron laboratory.

2. Gyrotron Components

A complete set of gyrotron modules (see Fig. 40) is stored for final assembly. Alternative modules are being constructed, in particular the thin-walled collector for beam measurements. The superconducting magnet system manufactured by industry failed to fulfill the specifications in three subsequent pre-tests at KfK. Nevertheless this magnet is being assembled with the cryostat for preliminary operation. A redesigned magnet will be constructed in the meantime. Parallel to the acceptance test of the magnet system, outbaking of the gyrotron modules and final assembly will be accomplished.

3. Gyrotron Theory

A nonlinear multimode code has been developed and applied to investigate the startup behavior with special emphasis on mode competition. Calculations including the pulse shape of the beam voltage show that multimode oscillation will occur in the present gun only at the maximum current.

Another code has been developed to cope with mode conversion in complex cavities. A system of coupled second order differential equations takes into account non principal modes and their effect on the efficiency of the gyrotron. A complex cavity to be inserted into the test gyrotron is being optimized by this new design method.

4. Microwave Diagnostics

The measurement systems for the frequency and mode spectra and for the integral microwave power have been constructed and are presently under test. The microwave measurement capability was improved by installation of a new carcinotron signal source delivering a power of 0.5 Watt in the range of 130 to 160 GHz. A multichannel spectrum analyzer is under construction to solve the real time measurement problem for the analysis of mode competition during transients.

Staff:
W. Baumgärtner
E. Borie
H. Budig
G. Dammertz
F. Graf
P. Grundel
G. Haubrich
R. Hietschold
G. Hochschild
A. Hornung
K. Jentzsch
B. Jödicke
M. Kuntze
R. Lehm
A. Möbius
N. Münch
H. Oppermann
B. Piosczyk
G. Redemann
H. Stickel
R. Vincon
H. Wenzelburger

External Contributors:

K. Behm and team	(Valvo, Hamburg)
E. Jensen et al.	(TU, Hamburg-Harburg)
M. Kitlinski et al.	(IHE, Univ. Karlsruhe)
M. Thumm et al.	(IPF, Univ. Stuttgart)
O. Dumbrajs	(Abas, Leopoldshafen)
C. Edgecombe	(Univ. Cambridge, UK)

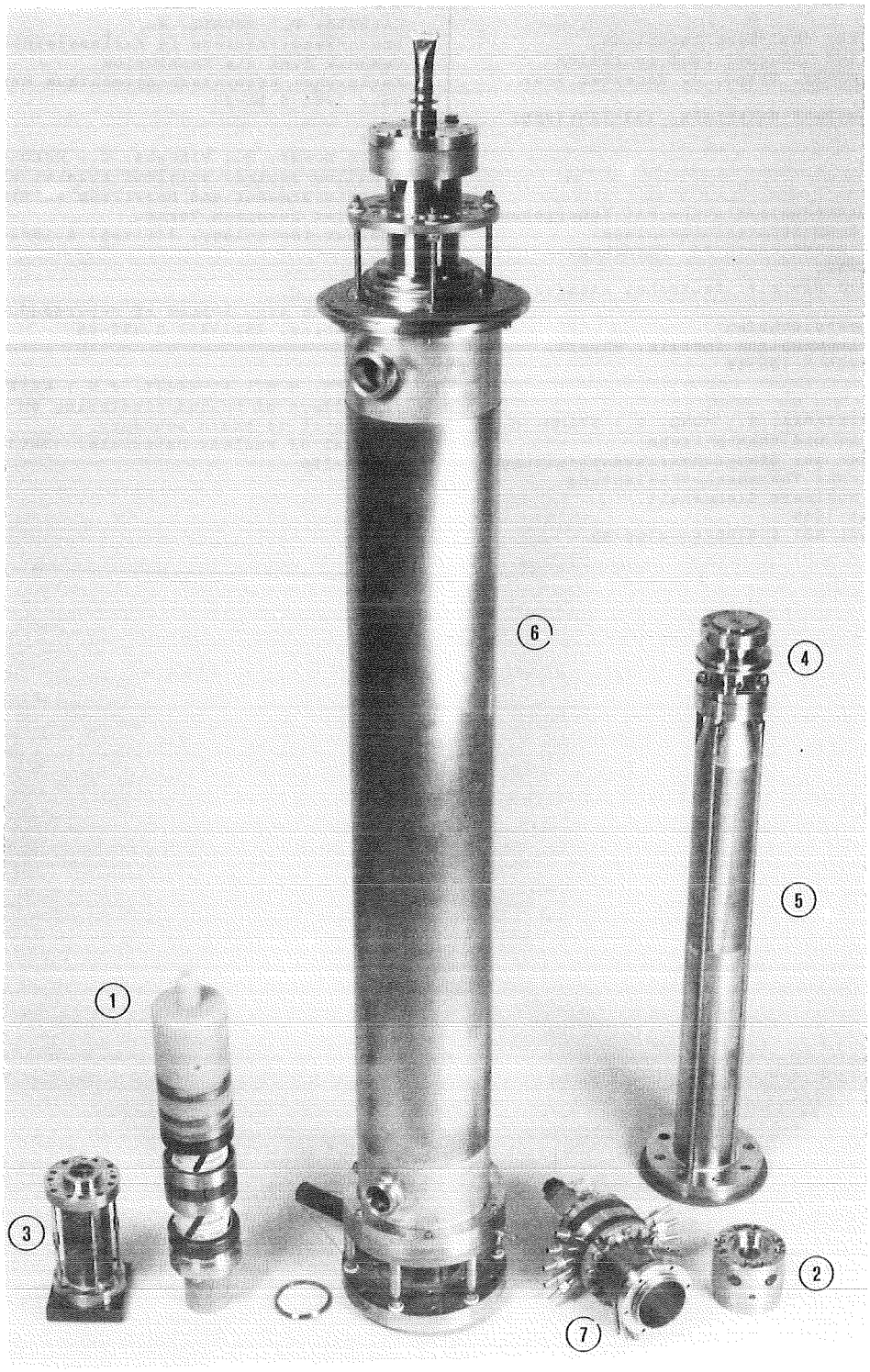

Fig. 40: Gyrotron modules before final assembly

1	hollow beam gun	5	output taper
2	valve	6	collection
3	input taper		
4	resonator		

20214 IMF;
KALETTA, D.
The high-energy dual-beam technique.
Proc.of the 1st Internat.Conf.on Fusion Reactor Materials, Tokyo, J, December 3-6, 1984
Journal of Nuclear Materials, 133+134(1985) S.878-81

21384 IMF;
KALETTA, D.
Einachsige Ermuedungsversuche mit Rohrproben an der Dual-Beam-Bestrahlungsanlage.
Jahrestagung Kerntechnik 85. Muenchen, 21.-23.Mai 1985.
Kerntechnische Ges.e.V. Deutsches Atomforum e.V.
Eggenstein-Leopoldshafen: Fachinformationszentrum Energie, Physik, Mathematik 1985 S.785-88

21395 IMF;
CZUCK, G.; RINTAMAA, R.; MUNZ, D.; STAMM, H.
Experimentelle und theoretische Untersuchungen zur Ermuedungsrissausbreitung unter zyklischer Thermoschockbelastung.
In: Projekt Nukleare Sicherheit.
Jahresbericht 1984
KfK-3550 (Juni 85) S.4100/44-4100/52

21495 IMF; ITP;
KALETTA, D.; MAURER, W.
Erste-Wand-Probleme im Fusionsreaktor.
Technik fuer die Kernfusion
Karlsruhe: Kernforschungszentrum Karlsruhe GmbH 1985 S.25-27

21911 INR;
DALLE DONNE, M.; FISCHER, U.; KUECHLE, M.
A helium-cooled, poloidal blanket with ceramic breeder and beryllium multiplier for the Next European Torus.
Nuclear Technology, 71(1985) S.15-28

21998 ITP;
SCHMIDT, C.
Measuring a.c. losses of superconductors.
Cryogenics, 25(1985) S.492-95

22398 IMF;
GHONIEM, N.M.; AL-HAJJI, J.N.; KALETTA, D.
The effect of helium clustering on its transport to grain boundary.
Journal of Nuclear Materials, 136(1985) S.192-206

V21244 ITP;
JESKE, U.; POLO-TEAM
A 4 MJ, 200 T/S pulsed ring coil. Status of the design and the test arrangements.
9th Internat.Conf.on Magnet Technology (MT-9), Zuerich, CH, September 9-13, 1985

V21327 IDT; ITP; IT;
JUENGST, K.P.; FRIESINGER, G.; GEIGER, W.; GRUENHAGEN, A.; KIESEL, H.; KOMAREK, P.; OBERMAIER, G.; SUESS, E.; YAN, L.
Superconducting torus 'TESPE' at design values.
9th Internat.Conf.on Magnet Technology (MT-9), Zuerich, CH, September 9-13, 1985

V21435 ITP;
SCHMIDT, C.; SCHWEIKERT, K.; SPECHT, E.
Test of a low loss superconductor for use in a poloidal field coil.
9th Internat.Conf.on Magnet Technology (MT-9), Zuerich, CH, September 9-13, 1985

V21436 ITP;
SPECKING, W.; NYILAS, A.; FLUEKIGER, R.
Strain sensitivity of subsize fusion conductor based on Nb_3Sn.
9th Internat.Conf.on Magnet Technology (MT-9), Zuerich, CH, September 9-13, 1985

V21460 INR;
DALLE DONNE, M.; FISCHER, U.; KUECHLE, M.
Some considerations on the protective layer for the NET first wall.
Meeting on First Wall Components, Culham, GB June 18-20, 1985

V21619 ITP;
TUROWSKI, P.
A 12 T NbTi solenoid at 1.8 K with 290 mm clear bore.
9th Internat.Conf.on Magnet Technology (MT-9), Zuerich, CH, September 9-13, 1985

V21796 ITP;
BARTH, W.; LEHMANN, W.; TUROWSKI, P.
Erfahrungen mit HeII-Kuehlung supraleitender Magnete - Verfahrens- und Kryotechnik.
DKV-Jahrestagung (Deutscher Kaelte- und Klimatechnischer Verein), Aachen, 20.-22.November 1985

V21800 ITP;
SCHMIDT, C.
Transient heat transfer into a closed volume of liquid helium.
1.Sowjetisch-Westdeutsches Symp.zur Waermeuebertragung in Kryosystemen, Kharkow, SU, 24.-27.September 1985

V21957 IMF; ITP;
NYILAS, A.; ZEHLEIN, H.
Theoretical and experimental studies of forming and failure of force flow cooled superconductor bends.
11th Symp.on Fusion Engineering, Austin, Tex., November 18-22, 1985

V22265 INR; IMF;
DALLE DONNE, M.; FISCHER, U.; BOJARSKY, E.; REISER, H.
Pebble bed canister: a ceramic breeder blanket design with radial helium cooling.
NET-Blanket Engineering Meeting on Solid Breeder Blankets, Karlsruhe, November 26-28, 1985

V22399 IMF;
KALETTA, D.; KRUEGER, TH.
A data acquisition system for the duel beam target station.
Internat.INTEREX/HP-1000 Users Conf., Antwerpen, B, April 9-12, 1985

V22407 ITP;
NYILAS, A.
Supraleitende Grossmagnete in der Fusionstechnologie unter Berucksichtigung von Werkstoffproblemen bei Strukturmaterialien.
Werkstoffkolloquium, Universitaet Karlsruhe, 17.Dezember 1985

Appendix I: Participation of KfK Departments in the Fusion Technology Programme

Task Code No.	Title	KfK Departments
B 1	Blanket Design Studies	Institute for Neutron Physics and Reactor Engineering (INR) Institute for Reactor Components (IRB) Institute for Materials and Solid State Research (IMF) Central Engineering Department (IT)
B 2	Development of Computational Tools for Neutronics	Institute for Neutron Physics and Reactor Engineering (INR)
B 6	Corrosion of Structural Materials in Flowing $Li_{17}Pb_{83}$	Institute for Materials and Solid State Research (IMF)
B 9	Tritium Extraction based on the Use of Solid Getters	Central Engineering Department (IT)
B 11 - B 16	Ceramic Breeder Materials	Institute for Materials and Solid State Research (IMF) Institute for Neutron Physics and Reactor Engineering (INR) Institute for Radiochemistry (IRCh)
M 1	The Large Coil Task (LCT)	Institute for Technical Physics (ITP) Institute for Data Processing in Technology (IDT)
M 3	Development of High Field Composite Superconductors	Institute for Technical Physics (ITP)
M 4	Superconducting Poloidal Field Coils	Institute for Technical Physics (ITP)
M 9	Structural Materials Fatigue Characterization at 4 K	Institute for Technical Physics (ITP)
M 12	Development of Low Electrical Conductivity Structures	Institute for Technical Physics (ITP) Institute for Materials and Solid State Research (IMF)
MAT 1.2	Pre- and Postirradiation Properties of 1.4914 Martensitic Steel	Institute for Materials and Solid State Research (IMF)
MAT 2.2	In-pile-creep-fatigue Testing of Type 316 and 1.4914 Steels	Institute for Materials and Solid State Research (IMF)
MAT 6/	Ceramics for First Wall Protection, Insulators and Windows	Institute for Materials and Solid State Research (IMF)
MAT 9.2	Investigation of Fatigue under Dual-Beam Irradiations	Institute for Materials and Solid State Research (IMF)

N 5	Development of Theory and Tools for Evaluation of Magnetic Fields Effects on Liquid Breeder Blanket	Institute for Reactor Components (IRB)
RM 3	Handling Equipment for In-Vessel Components	Institute for Neutron Physics and Reactor Engineering (INR)
S+E 1	Radioactive Effluents in the System Plant/Soil	Central Safety and Security Department (HS)
S+E 4.1.2	Safety Aspects of the Cryosystem	Institute for Neutron Physics and Reactor Engineering (INR)
S+E 4.1.3	Safety Aspects of Superconducting Magnets	Institute for Technical Physics (ITP) Institute for Data Processing in Technology (IDT)
T 6	Industrial Development of Large Components for Plasma Exhaust Pumping	Central Engineering Department (IT)
T 10 H	Plasma Exhaust Purification: Catalyst Development	Institute for Radiochemistry (IRCh)
	Development of ECRH Power Sources at 150 GHz	Institute for Nuclear Physics (IK) Institute for Data Processing in Technology (IDT)

Appendix II: Table of NET Contracts

Theme	Contract No.	Working Period
Stress and Lifetime Calculations for First Wall and Blanket Structural Components in NET	155/84-5/FU-D/NET	6/84 - 5/86
TF-Coil Design Contract	183/84-12/FU-D/NET	12/84 - 12/86
NET/INTOR Maintenance and Remote Handling Techniques-Support for Specific Tasks	193/85-2/FU-D/NET	2/85 - 12/85
Scoping Study on Structural Low Electrical Conductivity and Insulation Materials for NET Magnetic Systems	194/85-3/FU-D/NET	3/85 - 9/85
Availability of the LCT Plant	210/85-9/FU-D/NET	10/85 - 12/87
Availability of the TESPE Device	211/85-9/FU-D/NET	10/85 - 12/86

Appendix III: KfK Departments and Fusion Project Management Group

Kernforschungszentrum Karlsruhe GmbH
Postfach 3640
D-7500 Karlsruhe 1
Federal Republic of Germany
Telephone (07247) 82-1
Telex 7 826 484
Telefax/Telecopies (0)07247/82 5070

KfK Department	KfK Institut/Abteilung	Director	Tel.
Applied Systems Analyses Department	Abteilung für Angewandte Systemanalyse (AFAS)	Dr. H. Paschen	2500
Central Data Processing and Instrumentation Department	Hauptabteilung Datenverarbeitung und Instrumentierung (HDI)	DP. H. Stittgen	2462
Central Safety and Security Department	Hauptabteilung Sicherheit (HS)	Prof. Dr. H. Kiefer	2660
Institute for Data Processing in Technology	Institut für Datenverarbeitung in der Technik (IDT)	Prof. Dr. H. Trauboth	5700
Institute for Nuclear Physics	Institut für Kernphysik II (IK)	Prof. Dr. A. Citron	3502
Institute for Materials and Solid State Research	Institut für Material- und Festkörperforschung (IMF)	I. Prof. Dr. F. Thümmler II. Dr. K. Anderko III. Prof. Dr. K. Kummerer IV. Prof. Dr. D. Munz	2918 2902 2518 4815
Institute for Neutron Physics and Reactor Engineering	Institut für Neutronenphysik und Reaktortechnik (INR)	Prof. Dr. G. Keßler	2440
Institute for Reactor Components	Institut für Reaktorbau-elemente (IRB)	Prof. Dr. U. Müller	3450
Institute for Radiochemistry	Institut für Radiochemie (IRCH)	Prof. Dr. H.J. Ache	3200
Institute for Reactor Development	Institut für Reaktor-entwicklung (IRE)	Prof. Dr. D. Smidt	2550
Central Engineering Department	Hauptabteilung Ingenieur-technik (IT)	Dr. H. Rininsland	3001
Institute for Technical Physics	Institut für Technische Physik (ITP)	Prof. Dr. P. Komarek (acting)	2653
Nuclear Fusion Project - Project Management	Projekt Kernfusion Projektleitung (PKF-PL)	Dr. J.E. Vetter	5460
Secretary	I. Sickinger, I. Pleli		5461/5466
Administrator	Dr. D. Finken		5462
Blanket, Facilities	DI. H. Sebening		5464
Superconducting Magnets, ECR-Heating	N.N. (Dr. J.E. Vetter)		5460
Tritium, Materials	Dr. H.D. Röhrig		5463
Safety, Remote Handling	DI. A. Fiege		2668
System Studies	Prof. Dr. P. Komarek		2653